AGU PUBLICATIONS

Tectonics

RESEARCH ARTICLE
10.1002/2017TC004600

Key Points:
- The ~2592–2503 Ma episodic high-pressure TTGs to medium-/low-pressure TTGs and potassic granitoids from North China Craton
- Magmatic evolution indicates periodic crustal thickening and thinning, marking crustal formation and stabilization in an accretionary orogen
- Contribution of accretionary orogens to late Archean continental growth and stabilization

Supporting Information:
- Supporting Information S1
- Supporting Information S2
- Figure S1
- Figure S2
- Figure S3
- Figure S4
- Figure S5
- Figure S6
- Figure S7
- Table S1
- Table S2
- Table S3
- Table S4

Correspondence to:
W. Wang and S. Liu,
wangw1988@cugb.edu.cn;
sanyechong198819@163.com;
swliu@pku.edu.cn

Citation:
Wang, W., P. A. Cawood, S. Liu, R. Guo, X. Bai, and K. Wang (2017), Cyclic formation and stabilization of Archean lithosphere by accretionary orogenesis: Constraints from TTG and potassic granitoids, North China Craton, *Tectonics*, *36*, doi:10.1002/2017TC004600.

Received 5 APR 2017
Accepted 17 JUL 2017
Accepted article online 27 JUL 2017

Cyclic formation and stabilization of Archean lithosphere by accretionary orogenesis: Constraints from TTG and potassic granitoids, North China Craton

Wei Wang[1,2,3], Peter A. Cawood[3,4], Shuwen Liu[2], Rongrong Guo[5], Xiang Bai[6], and Kang Wang[2]

[1]The State Key Laboratory of Geological Processes and Mineral Resources, School of Earth Sciences and Resources, China University of Geosciences, Beijing, China, [2]The Key Laboratory of Orogenic Belts and Crustal Evolution, Ministry of Education, School of Earth and Space Sciences, Peking University, Beijing, China, [3]Department of Earth Sciences, University of St. Andrews, St. Andrews, UK, [4]School of Earth, Atmosphere and Environment, Monash University, Melbourne, Victoria, Australia, [5]Department of Geology, College of Resources and Civil Engineering, Northeastern University, Shenyang, China, [6]Key Laboratory of Active Tectonics and Volcano, Institute of Geology, China Earthquake Administration, Beijing, China

Abstract Accretionary orogens are major sites of modern continental growth, yet their role in the development of Archean continental crust remains enigmatic. Diverse granitoid suites from tonalite-trondhjemite-granodiorite (TTG) to potassic granitoids appeared during late Archean, representing a period of major continental formation and stabilization. In this study, whole-rock geochemical and zircon U-Pb and Lu-Hf isotopic data are reported for Neoarchean granitoid gneisses from the Northern Liaoning Terrane, northeastern North China Craton (NCC). Older granitoid gneisses (~2592–2537 Ma) define three magmatic zones migrating from southeast to northwest, each showing a common magmatic evolution from high-pressure TTGs to medium-/low-pressure TTGs and potassic granitoids. They have depleted zircon $\varepsilon Hf(t)$ of +0.5 to +8.7. Younger ~2529–2503 Ma potassic granitoids and TTGs occur throughout the terrane, which are marked by variable zircon $\varepsilon Hf(t)$ of −4.7 to +8.1, and are coeval with regional high-grade metamorphism. Petrogenetic modeling and changing Sr/Y and $(La/Yb)_N$ of the granitoids suggest that the crust experienced episodic thickening and thinning and became progressively evolved through development of potassic granitoids and sedimentary successions. The metavolcanic basement to the granitoids display tholeiitic to calc-alkaline affinities, together with the top-to-the-northwest thrusting and associated volcanogenic massive sulfide-type Cu-Zn deposits, suggesting cyclic crustal formation of Northern Liaoning within an accretionary orogen with a SE-dipping subduction polarity. Cyclic crustal thickening and thinning is related to tectonic switching from advancing to retreating relations between the downgoing and overriding plate. After ~2530 Ma, this accretionary system accreted to the ancient continental nucleus of NCC (Anshan-Benxi Terrane), signifying final lithosphere stabilization.

1. Introduction

Accretionary orogens form at sites of convergent plate interaction and have been major sites of continental growth throughout the Neoproterozoic and Phanerozoic (e.g., Central Asian Orogenic Belt, the Arabian-Nubian Shield, and the circum-Pacific accretionary system) [*Cawood et al.*, 2009]. Granitoid rocks within accretionary orogens form during plate convergence as well as subsequent collision and stabilization of the plate margin, and provide a record of continental crust formation and its subsequent incorporation into the geological archive [*Jahn et al.*, 2000; *Kemp et al.*, 2009; *Phillips et al.*, 2011; *Robinson et al.*, 2014]. The role of accretionary orogens and indeed plate tectonics during the Archean and Hadean is debated [e.g., *Cawood et al.*, 2006; *Korenaga*, 2013] but is crucial in understanding the evolution of the continental crust as some 70% or more of this crust is estimated to have formed at this time [*Foley et al.*, 2002; *Cawood et al.*, 2013; *Santosh et al.*, 2013; *Hawkesworth et al.*, 2016].

Sodic tonalite-trondhjemite-granodiorite (TTG) and potassic granitoid gneisses are major components of Archean continental crust and preserve valuable information about Early Precambrian planetary differentiation and continental growth [*Martin et al.*, 2005, 2014; *Moyen*, 2011, *Moyen and Martin*, 2012; *Condie*, 2014; *Laurent et al.*, 2014; *Halla et al.*, 2017]. In this paper, we document a record of crustal evolution involving Neoarchean granitoid gneisses from Northern Liaoning Terrane (NLT) of northeastern North China Craton (NCC, Figure 1). The gneisses display a laterally repeated record evolving from high-pressure TTGs to

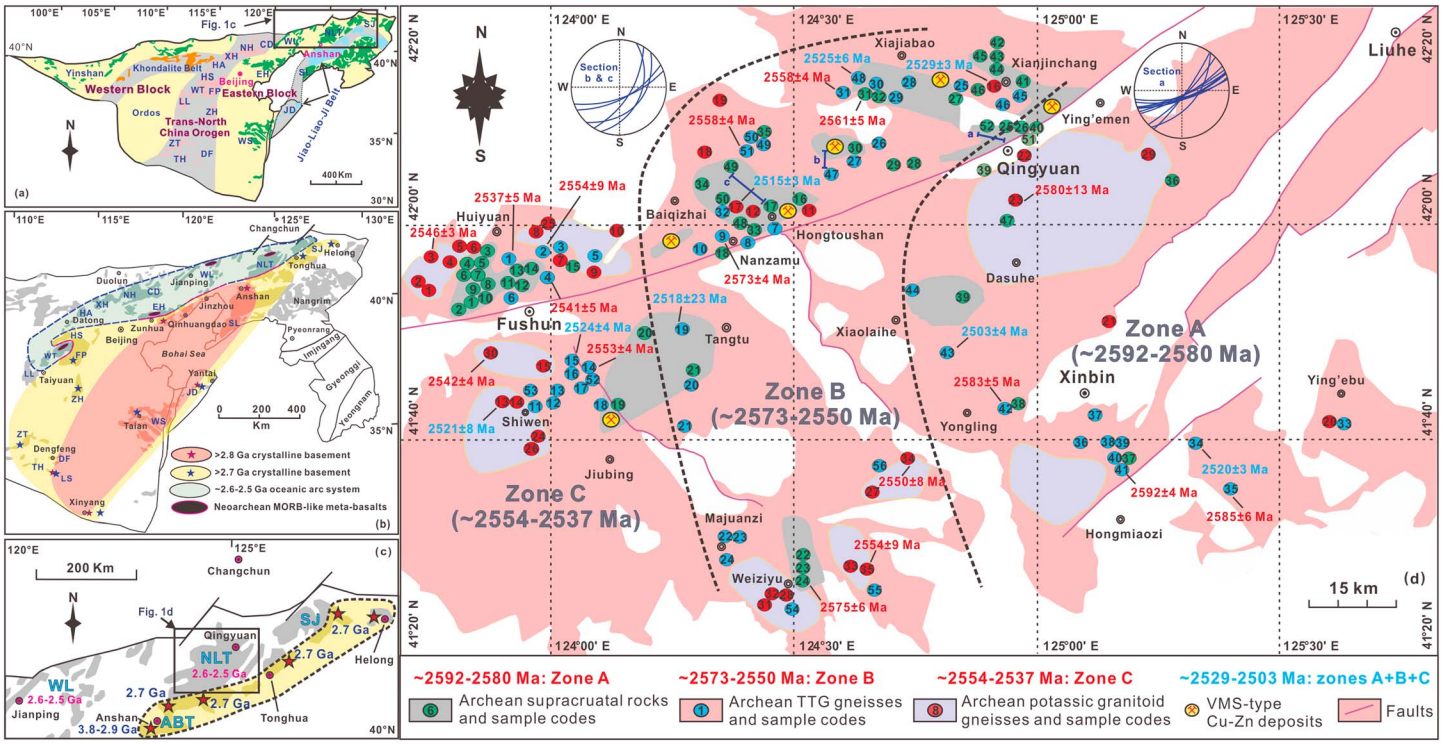

Figure 1. Simplified geological maps of the (a) late Paleoproterozoic [*Zhao et al*., 2012] and (b) Archean [*Wang et al*., 2015] tectonic framework of North China Craton, showing (c, d) distribution of Northern Liaoning Terrane (NLT) in the northeastern segment of the Eastern Block. Neoarchean basement rocks of the Northern Liaoning Terrane are divided into three zones (A, B, and C), recording magmatic migration from southeast to northwest before 2530 Ma (~2592-2537 Ma). Sample codes and ages are listed in Figure 1d and referred to Tables 1 and S2. Structural analyses of three cross sections straddling or near the proposed tectonic boundaries among different magmatic zones (section a: 42°07′35″N, 124°57′36″E to 42°08′12″N, 124°57′06″E; section b: 42°04′56″N, 124°33′36″E to 42°05′55″N, 124°33′23″E; and section c: 42°01′44″N, 124°31′05″E to 42°01′43″N, 124°30′59″E) show dominantly high angle SE-dipping foliation (lower hemisphere projection on a Wulff net). The locations of volcanogenic massive sulfide (VMS) Cu-Zn deposits are also shown [*Zhu et al*., 2015]. CD, Chengde; DF, Dengfeng; EH, Eastern Hebei; FP, Fuping; HA, Huai'an; HS, Hengshan; JD, Jiaodong; LL, Lvliang; NH, Northern Hebei; SL, Southern Liaoning; TH, Taihua; WL, Western Liaoning; WT, Wutai; WS, Western Shandong; XH, Xuanhua; ZH, Zanhuang; ZT, Zhongtiao.

medium-/low-pressure TTGs and potassic granitoids, signifying a cycle of crustal formation, development, and final stabilization. The gneisses were emplaced into metavolcanic rocks with geochemical signatures indicative of arc-back arc systems and thus may represent part of an Archean accretionary orogen. This study outlines the geodynamic regime of late Archean granitoid formation and its role in continental growth and stabilization.

2. Geological Background

The North China Craton is one of the oldest cratons in the world [*Zhai and Santosh*, 2011; *Wan et al*., 2013]. Models for its final stabilization range from late Archean to Paleoproterozoic. The later models favor collision between Eastern and Western Blocks along trans-North China Orogen at ~1.85 Ga during assembly of the Nuna (Columbia) supercontinent (Figure 1a) [*Liu et al*., 2006; *Zhao et al*., 2012], whereas *Kusky* [2011] argued that the two separate blocks were amalgamated at the end of the Archean. *Zhai and Santosh* [2011] divided the Archean crystalline basement of North China Craton into seven blocks (Jiaoliao, Qianhuai, Xuhuai, Xuchang, Jining, Ordos, and Alashan), which were considered to have amalgamated largely along the greenstone belts during the late Archean. Recently, Kusky and coauthors suggested that crustal growth in the North China Craton occurred in a sequential, clockwise direction through the development of a series of sutures at 2.7 Ga, 2.5 Ga, 2.43 Ga, 2.3 Ga, and 1.9 Ga [*Kusky et al*., 2016]. A major ~2.5 Ga suture zone constitutes the Central Orogenic Belt, which records final end Archean collision between the N-S trending late Archean Wutai/Fuping arc and the Eastern Block [*Deng et al*., 2014]. Basement rocks in the Eastern Block have yielded ages mainly in the range of ~2.6 to 2.5 Ga with subordinate dates at ~2.7 Ga, along with some ~3.8 to

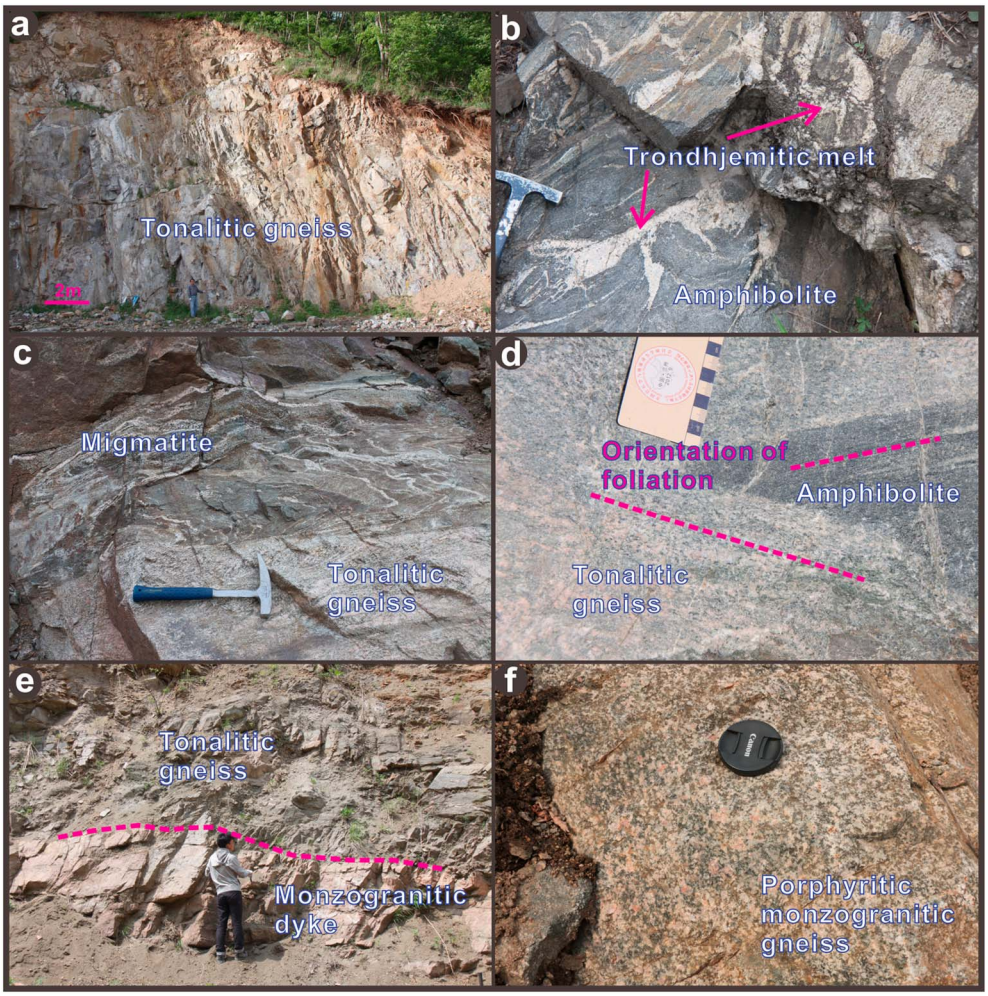

Figure 2. Field photographs for Archean crystalline basement of Northern Liaoning Terrane, illustrating (a) large-scale tonalitic gneisses; (b) incipient trondhjemitic melts within amphibolites with associated garnet-rich residues; (c) tonalitic gneisses intruding migmatized metavolcanic rocks; (d) angular amphibolite xenolith within tonalitic gneisses, with different foliation orientations; (e) monzogranitic dyke intruding tonalitic gneisses; and (f) porphyritic monzogranitic gneisses. The geologist, hammer, and lens cap as scale bars are 175 cm, 30 cm, and 8 cm, respectively.

2.8 Ga crustal relics [*Nutman et al*., 2011; *Zhai and Santosh*, 2011; *Wan et al*., 2014; *Guo et al*., 2016]. Based on the temporal and spatial distribution of rock units and their geochemical signatures, *Wang et al*. [2015] proposed a tectonic setting of a Neoarchean suprasubduction zone developed along the northwestern margin of the Eastern Block (Figure 1b).

The northeastern portion of the Eastern Block includes the ~3.8–2.5 Ga Anshan-Benxi Terrane in the southwest and ~2.7–2.5 Ga Southern Jilin and Northern Liaoning terranes in the northeast (Figure 1c) [*Wan et al*., 2013; *Guo et al*., 2016]. The Northern Liaoning Terrane is dominated by ~2.6–2.5 Ga biotite- or hornblende-bearing tonalitic and trondhjemitic gneisses (Figures 1d and 2a), with pyroxene-bearing TTG and dioritic gneisses locally developed. Metamorphosed volcano-sedimentary rocks in the terrane consist of (garnet) amphibolites, hornblende plagioclase gneisses (with less hornblende than amphibolites), biotite plagioclase gneisses, and locally hornblende two pyroxene granulites, with interlayered sillimanite biotite gneisses, banded iron formations, and marbles. Volcanogenic massive sulfide (VMS) Cu-Zn deposits are well developed in the Qingyuan-Xiajiabao, Hongtoushan, Baiqizhai, and Jiubing areas (Figure 1d) [*Zhu et al*., 2015, and references therein], which could have been formed in an intra-arc or back-arc basin settings [*Huston et al*., 2010; *W. Wang et al*., 2016]. Minor mid-ocean ridge basalt (MORB)-type metavolcanic rocks were identified in the Xiaolaihe area of Northern Liaoning Terrane [*Wan et al*., 2005; *Wang et al*., 2015]. They may

represent relict MORB-type oceanic crust, but no typical ophiolites have been recognized in the study region. Veins of incipient trondhjemitic and tonalitic melts are common in the metavolcanic rocks, associated with garnet-rich residues and migmatites (Figure 2b). The TTG gneisses intrude a regional succession of supracrustal rocks and contain metavolcanic xenoliths (Figures 2c and 2d). Potassic granitoids are locally developed (e.g., Dasuhe, Hongmiaozi, Weiziyu, and Huiyuan) and intrude TTG gneisses and metavolcanic rocks (Figures 1d and 2e). They are mainly fine- to coarse-grained monzo-/syenogranitic gneisses, with some porphyritic varieties and minor granodiorites (Figure 2f). Amphibolite and locally granulite facies metamorphism was coeval with the later stages of potassic granitoid intrusions [*W. Wang et al*., 2016].

Four deformation events have been recognized in the Northern Liaoning Terrane [*Shen et al*., 1994]. The first episode (D_1) is characterized by a regional penetrative foliation (S_1), mineral stretching lineation (L_1), and small-scale tight isoclinal folds (F_1). D_2 is the major deformation event in the study region, forming larger-scale asymmetric folds (F_2) as well as several ductile shear zones (e.g., in the Qingyuan area). Notably, the D_2 episode defines the regional NE-SW trending structural pattern. The third episode (D_3) is marked by large-scale N-S trending open folds (F_3) with local development of crenulation cleavage, showing transition from ductile to brittle deformation. The last episode (D_4) is mainly brittle in nature, forming dominantly NW trending symmetric broad folds (F_4) and normal faults. Our structural analyses across representative supracrustal rock series in the Qingyuan (section a) and Hongtoushan (sections b and c) areas indicate a high-angle SE-dipping foliation (lower hemisphere projection on a Wulff net, Figures 1d and S1a in the supporting information). Locally, the supracrustal succession displays a mylonitic fabric with SE-plunging mineral stretching lineation (Figure S1b). These structural features are consistent with the dominant NE-SW trending structural pattern in the study region [*Shen et al*., 1994], which when combined with the occurrence of asymmetric folds within the metavolcanic rock sequences, indicating strong ductile shear deformation and top-to-the-northwest thrusting (Figures S1c and S1d).

3. Sampling and Analytical Methods

Samples of 52 metavolcanic rocks, 69 TTG gneisses, and 35 potassic granitoid gneisses from the Northern Liaoning Terrane were selected for whole-rock major and trace element analyses by X-ray fluorescence (XRF) and inductively coupled plasma mass spectrometry (ICPMS). Laser ablation (LA)-ICPMS zircon U-Pb isotopic dating was performed on 27 samples, and results for 14 representative samples are presented in the main text (Figures 3 and 4). The complete data set is shown in Table 1 and Figure S2. Zircon Lu-Hf isotopes were determined by LA-Multi-collector (MC)-ICPMS on 25 dated samples. The analytical results along with details of the analytical procedures are listed in Tables S1–S3.

4. Zircon U-Pb and Lu-Hf Isotopes

4.1. Chronology of Metavolcanic Rocks

Metavolcanic rocks contain small, oval to stubby zircon grains. Cathodoluminescence (CL) images reveal a range of internal structures including banded or oscillatory zoning, as well as structureless or fir tree-zoned grains enveloped occasionally by bright rims (Figure 3).

Twenty-five spots were analyzed for samples 13LB27-1, 12LN39-3, and W15FS11-4, whereas 14 analyses were undertaken on sample 12LN76-2. Th/U ratios are mostly in the range 0.10–1.81, with values of 0.05–0.06 for spots W15FS11-4-08/-19/-20. $^{207}Pb/^{206}Pb$ ages of sample 13LB27-1 fall into two groups, yielding an older weighted mean $^{207}Pb/^{206}Pb$ age of 2550 ± 18 Ma (mean square weighted deviation (MSWD) = 0.032) and a younger upper intercept age of 2508 ± 10 Ma (MSWD = 0.068). Data for sample W15FS11-4 give a weighted mean $^{207}Pb/^{206}Pb$ age of 2525 ± 16 Ma (MSWD = 0.062), with 21 analyses showing a concordia age of 2525 ± 4 Ma (MSWD = 0.006). Considering the metamorphic zircon-like internal structures, the ages of 2550 Ma, 2525 Ma, and 2508 Ma are taken as timing of metamorphic events. Analyses from samples 12LN76-2 and 12LN39-3 define discordia lines. The concordant analyses yield weighted mean $^{207}Pb/^{206}Pb$ ages of 2562 ± 17 Ma (MSWD = 0.07) for 12LN76-2 and 2552 ± 48 Ma (MSWD = 0.038) for 12LN39-3, and concordia ages of 2561 ± 5 Ma (MSWD = 0.002) and 2575 ± 6 Ma (MSWD = 0.84), respectively. Given magmatic zircon-like CL structures, the concordia ages of 2561 Ma and 2575 Ma are taken as crystallization ages of their magmatic precursors.

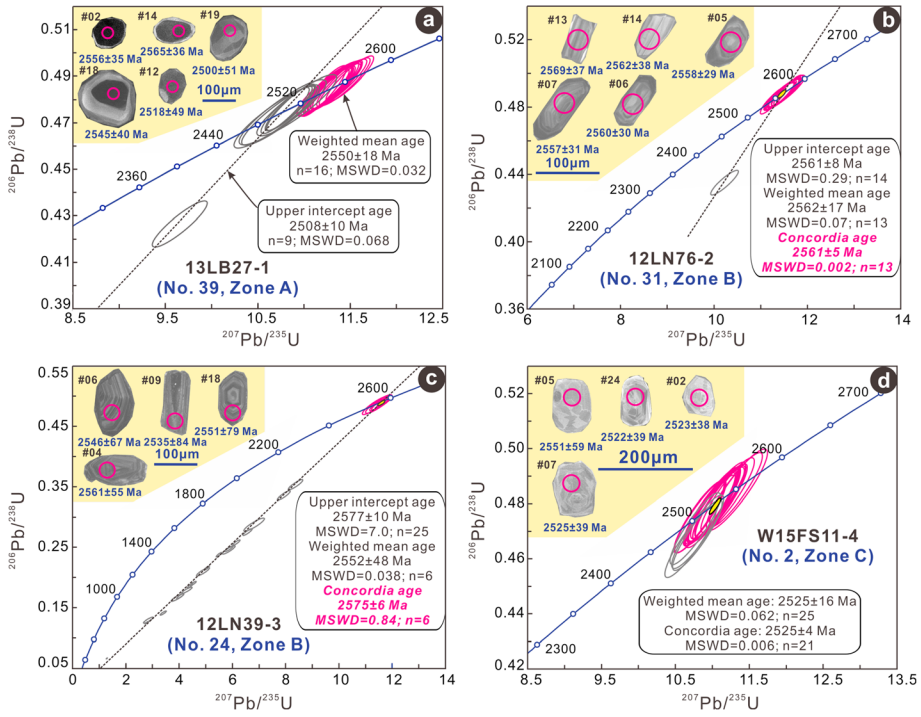

Figure 3. Concordia plots of zircon U-Pb isotopic dating data and calculated ages for metavolcanic rocks from Northern Liaoning Terrane: hornblende plagioclase gneiss samples (a) 13LB27-1 and (c) 12LN39-3; and amphibolite samples (b) 12LN76-2 and (d) W15FS11-4. The insets are CL images of internal structures and ages for representative zircon grains of each sample. Sample codes and locations are shown in the brackets.

The mafic volcanic rocks at Hongtoushan and Tangtu areas yield crystallization ages of ~2571 Ma and ~2530 Ma, both with metamorphic imprints at ~2508 Ma [*Bai et al*., 2014; *Zhu et al*., 2015]. In summary, basaltic to andesitic rocks of Northern Liaoning Terrane erupted at ~2570–2530 Ma or earlier and record metamorphism at ~2550 Ma and ~2525–2508 Ma.

4.2. Chronology of TTG Gneisses

Zircon grains from the tonalitic to trondhjemitic gneisses are stubby to elongate, and most exhibit oscillatory to banded zoning on CL images (Figures 4a–4f). Some grains have core-rim structures showing: (1) oscillatory zoned cores enveloped by dark rims (e.g., 13LB16-4-03); (2) structureless cores surrounded by bright or dark rims (e.g., 13LB13-1-20); or (3) oscillatory zoned or structureless cores with oscillatory zoned rims (e.g., 13LB47-3-10).

Twenty-five spots were analyzed for samples 13LB16-4, W15FS69-2, 13LB47-3, W15FS45-1, and W15FS31-1, except for 24 analyses for sample 13LB13-1. Th/U ratios range mostly from 0.10 to 1.76, with lower values of 0.02–0.09 for spots 13LB16-4-02/-19, 13LB47-3-03/-06/-09/-13/-23, W15FS45-1-01/-02/-06/-15/-20/-21, and W15FS31-1-08/-09/-14/-20/-22. Six analyses on structureless cores of sample 13LB13-1 (#08, #14, #20, #22, #23, and #24) yield an upper intercept age of 2635 ± 12 Ma (MSWD = 0.094). Eight analyses of oscillatory zoned cores from sample 13LB47-3 (#02, #04, #07, #08, #10, #12, #19, and #22) show $^{207}Pb/^{206}Pb$ ages of 2712–2594 Ma, with the six younger analyses yielding a weighted mean $^{207}Pb/^{206}Pb$ age of 2608 ± 16 Ma (MSWD = 0.28). One banded zoned grain from sample W15FS31-1 (#07) gives a $^{207}Pb/^{206}Pb$ age of 2583 ± 19 Ma. These ages are older than the main age group of magmatic zircons for each sample and are taken as ages of xenocrystic zircons. Two analyses (#01 and #02) on dark rims of sample 13LB16-4 show younger $^{207}Pb/^{206}Pb$ ages of 2532–2527 Ma, which could represent the timing of a metamorphic event. The remaining analyses for each of the six dated samples yield concordia ages of 2592 ± 4 Ma (MSWD = 0.017) for sample 13LB16-4, 2585 ± 6 Ma (MSWD = 0.005) for sample 13LB13-1, 2573 ± 4 Ma (MSWD = 0.009) for sample W15FS69-2, 2558 ± 4 Ma (MSWD = 0.021) for sample 13LB47-3, 2541 ± 5 Ma (MSWD = 0.016) for sample W15FS45-1, and 2537 ± 5 Ma (MSWD = 0.001) for sample W15FS31-1 (Figures 4a–4f). The concordia age of each sample is within error of the upper intercept age from discordia

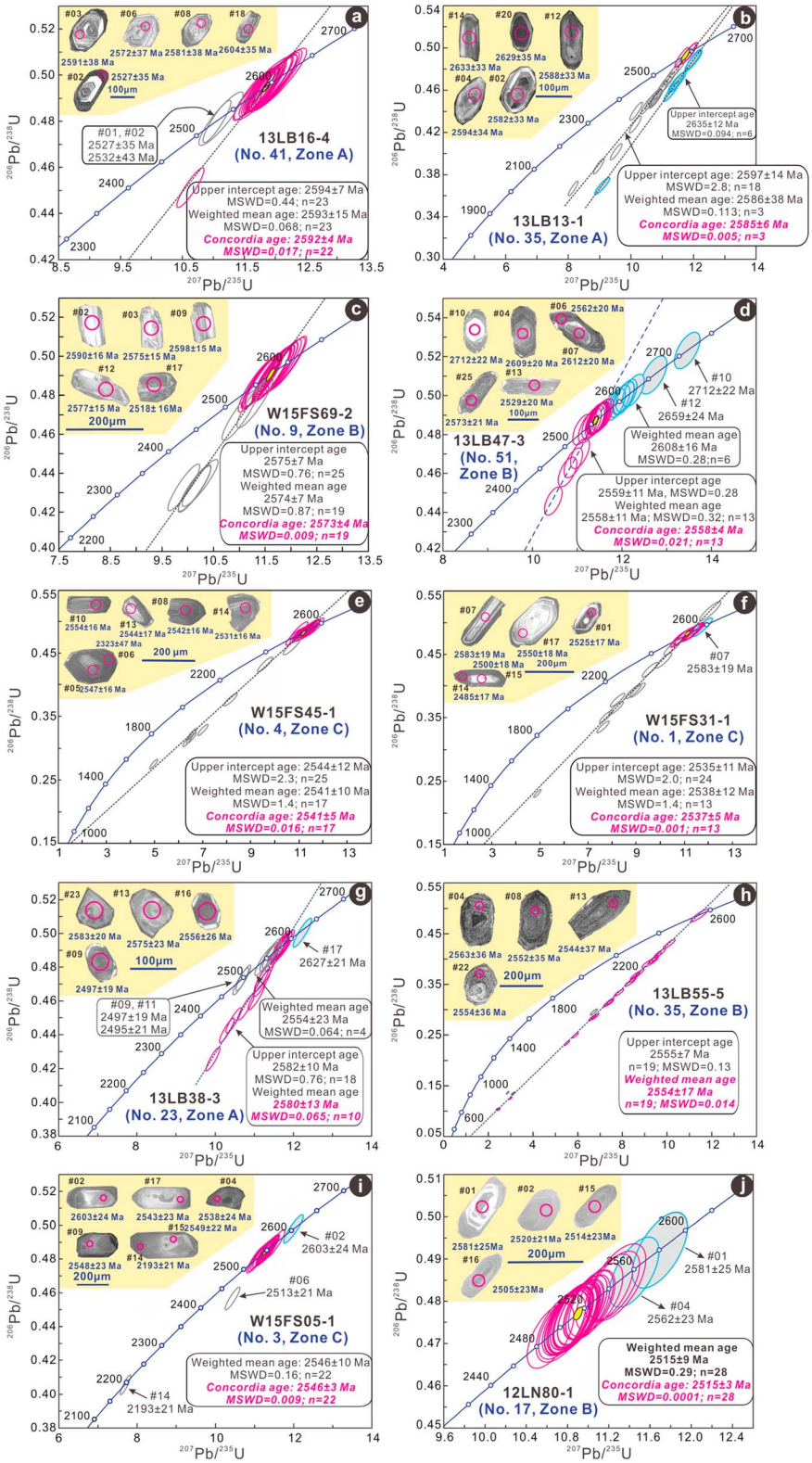

Figure 4. Concordia plots of zircon U-Pb isotopic dating data and calculated ages for representative (a–f) TTG and (g–j) potassic granitoid gneisses from Northern Liaoning Terrane. Note that pre-2530 Ma granitoid magmatism occurred during ~2592–2580, ~2573–2550, and ~2554–2537 Ma within zones A, B, and C, respectively. The insets are CL images of internal structures and ages for representative zircon grains of each sample. Sample codes and locations are shown in the brackets.

Table 1. Summary of Zircon U-Pb Isotopic Ages, Major Geochemical Parameters, and Petrogenesis of Archean Basement Rocks in the Northern Liaoning Terrane[a]

Sample (Code)	Lithological Units	SiO_2 (%)/MgO (%)/$(La/Yb)_N$/Sr/Y	Petrogenesis	Crystallization Age (Ma)	Xenocrystic Zircon Age (Ma)	Metamorphic Age (Ma)	References
			Pre-2530 Ma Magmatic Episode (2592–2537 Ma)				
			Zone A (~2592–2580 Ma)				
13LB16-4 (41)	Hongmiaozi trondhjemitic gneiss	69.10/0.82/ 28.29/143.13	HP melting of metabasalts	2592 ± 4		2532 ± 43/ 2527 ± 35	This study
13LB13-1 (35)	Hongmiaozi trondhjemitic gneiss	69.42/1.21/ 19.38/110.55	MP melting of metabasalts	2585 ± 6	2635 ± 12		This study
13LB25-2 (42)	Xinbin trondhjemitic gneiss	65.70/1.45/ 24.63/43.32		2583 ± 5		2487 ± 5	*M. J. Wang et al.* [2016]
13LB38-3 (23)	Dasuhe monzogranitic gneiss	64.22/1.82/ 21.40/11.56	LP melting of metaandesites	2580 ± 13	2627 ± 21	2554 ± 23/ 2497 ± 19/ 2495 ± 21	This study
13LB27-1 (39)	Dasuhe amphibolite		Partial melting of a hydrous mantle source metasomated by slab fluids	>2550		2550 ± 18/ 2508 ± 10	This study
			Zone B (~2573–2550 Ma)				
12LN39-3 (24)	Weiziyu hornblende plagioclase gneiss		Partial melting of a hydrous mantle source metasomated by slab fluids and melts	2575 ± 6			This study
W15FS69-2 (9)	Hongtoushan tonalitic gneiss	71.00/2.21/ 2.34/4.75	LP melting of metabasalts	2573 ± 4			This study
12LN76-2 (31)	Xiajiabao amphibolite		Partial melting of a hydrous mantle source metasomated by slab fluids	2561 ± 5			This study
12LN78-1 (31)	Xiajiabao trondhjemitic gneiss	71.56/0.70/ 12.19/98.01		2558 ± 4	2592 ± 20		*W. Wang et al.* [2016]
13LB47-3 (51)	Baiqizhai trondhjemitic gneiss	69.94/0.87/ 72.29/164.31	HP melting of metabasalts	2558 ± 4	2712 ± 22/ 2659 ± 24/ 2608 ± 16		*W. Wang et al.* [2016]
15LB29-1 (34)	Weiziyu monzogranitic gneiss	69.71/0.77/ 154.71/93.85	MP melting of metaandesites and metagreywackes	2550 ± 8	2581 ± 17	2515 ± 9	This study
13LB55-5 (35)	Weiziyu syenogranitic gneiss	68.40/0.66/ 79.17/80.61		2554 ± 17			This study
			Zone C (~2554–2537 Ma)				
W15FS39-1 (2)	Huiyuan tonalitic gneiss	71.39/1.31/ 29.08/89.96	HP melting of metabasalts	2554 ± 3			This study
12LN15-1 (14)	Shiwen trondhjemitic gneiss	67.54/2.18/ 13.76/45.08		2553 ± 4	2584 ± 10	2522 ± 8	*W. Wang et al.* [2016]
W15FS45-1 (4)	Huiyuan trondhjemitic gneiss	67.59/1.58/ 10.94/34.00	MP melting of metabasalts	2541 ± 5			This study
W15FS31-1 (1)	Huiyuan tonalitic gneiss	66.88/1.56/ 15.97/53.14		2537 ± 5	2583 ± 19		This study
W15FS05-1 (3)	Huiyuan syenogranitic gneiss	78.48/0.02/ 38.20/51.90	HP melting of metamorphosed andesites, greywackes, and pelites	2546 ± 3	2603 ± 24	2513 ± 21/ 2193 ± 21	This study
15LB04-1 (30)	Shiwen granodioritic gneiss	63.85/2.20/ 16.34/76.78		2542 ± 4			Our unreported data
W15FS11-4 (2)	Fushun amphibolite		Partial melting of a mantle source without subduction metasomatism	>2525		2525 ± 4	This study
			<2530 Ma Magmatic Episode (Covering Whole Northern Liaoning Terrane)				
12LN59-1 (16)	Xianjinchang monzogranitic gneiss	71.17/0.95/ 46.14/25.40	MP to HP melting of mixed sources of metamorphosed	2529 ± 3	2778 ± 54/ 2623 ± 54/ 2558 ± 54	2495 ± 38	*W. Wang et al.* [2016]
12LN01-1 (13)	Shiwen monzogranitic gneiss	66.47/1.35/ 44.82/164.18	andesites, TTG, and greywackes, with	2521 ± 8			*Bai et al.* [2014]

Table 1. (continued)

Sample (Code)	Lithological Units	SiO_2 (%)/MgO (%)/$(La/Yb)_N$/Sr/Y	Petrogenesis	Crystallization Age (Ma)	Xenocrystic Zircon Age (Ma)	Metamorphic Age (Ma)	References
12LN80-1 (17)	Hongtoushan monzogranitic gneiss	72.37/0.70/6.83/66.01	involvement of early Archean crustal materials	2515 ± 3	2581 ± 25/2562 ± 23		*W. Wang et al.* [2016]
13LB46-5 (48)	Xiajiabao trondhjemitic gneiss	70.56/0.72/5.13/43.57	HP melting of metabasalts	2525 ± 6	2646 ± 23/2592 ± 21	2498 ± 13	*W. Wang et al.* [2016]
12LN16-1 (15)	Shiwen trondhjemitic gneiss	69.80/1.56/13.59/57.07	MP melting of metabasalts	2524 ± 4		2496 ± 15	This study
13LB12-3 (34)	Hongmiaozi tonalitic gneiss	66.79/2.28/7.98/19.13	LP melting of metabasalts	2520 ± 3			This study
12LN27-1 (19)	Tangtu tonalitic gneiss	66.02/2.13/22.82/47.15	LP melting of metabasalts	2518 ± 23		2473 ± 30	*Bai et al.* [2014]
13LB26-5 (43)	Xiaolaihe trondhjemitic gneiss	67.42/1.46/15.54/86.90	HP melting of metabasalts	2503 ± 4	2559 ± 22/2553 ± 26		*W. Wang et al.* [2016]

[a]Sample codes are the same to those labeled in Figure 1d and Table S1. HP, high pressure; MP, medium pressure; LP, low pressure. The prefix "meta" is implicit for the basaltic to andesitic and sedimentary sources.

and the weighted mean $^{207}Pb/^{206}Pb$ age, and they are taken as the crystallization ages of the magmatic precursors for the tonalitic to trondhjemitic gneisses.

Another nine tonalitic to trondhjemitic gneiss samples yield crystallization ages between 2583 and 2503 Ma, with evidence for metamorphic events at ~2522 Ma and ~2498–2473 Ma based on zircon structures (Table 1 and Figure S2). In summary, the analyzed tonalitic to trondhjemitic gneisses from Northern Liaoning Terrane crystallized between 2592 and 2503 Ma and record metamorphism during ~2530–2470 Ma.

4.3. Chronology of Potassic Granitoid Gneisses

The long prismatic or stubby to irregular zircon grains from the monzogranitic to syenogranitic gneisses are mostly oscillatory zoned but with minor dark homogeneous grains (Figures 4g–4j). Some grains contain structureless cores or are surrounded by dark or bright rims.

Twenty-five spots were analyzed for samples 13LB38-3, 13LB55-5, and W15FS05-1 and 30 analyses for sample 12LN80-1. Th/U ratios are mostly 0.10–1.68, with values of 0.01–0.09 for spots 13LB38-3-03/-06/-10/-12, 13LB55-5-03/-05, W15FS05-1-14, and 12LN80-1-03/-30. Spots 13LB38-3-17, W15FS05-1-02, and 12LN80-1-01/-04 yield $^{207}Pb/^{206}Pb$ ages of 2627–2562 Ma. They are older than the main age group of each sample, and are interpreted as xenocrystic zircons. Six analyses on dark structureless grains from sample 13LB38-3 (#03, #06, #09, #11, #14, and #16) yield four older ages with a weighted mean age of 2554 ± 23 Ma (MSWD = 0.064) and two ages in the range 2497–2495 Ma. Spots W15FS05-1-06/-14 on dark rims give ages of 2513–2193 Ma. These younger analyses are therefore interpreted to record ages of metamorphic events. The remaining analyses for each sample were conducted on oscillatory zoned grains. Upper intercept ages of 2582 ± 10 Ma (MSWD = 0.76) and 2555 ± 7 Ma (MSWD = 0.13) are defined for samples 13LB38-3 and 13LB55-5, respectively, which are within error of the weighted mean ages of 2580 ± 13 Ma (MSWD = 0.065) and 2554 ± 17 Ma (MSWD = 0.014) for the two samples. Concordia ages of 2546 ± 3 Ma (MSWD = 0.009) and 2515 ± 3 Ma (MSWD = 0.0001) are calculated for samples W15FS05-1 and 12LB80-1, respectively, and they are within error of the weighted mean ages of 2546 ± 10 Ma (MSWD = 0.16) and 2515 ± 9 (MSWD = 0.29) for the two samples.

Four other monzogranitic to granodioritic gneiss samples show crystallization ages between 2550 and 2521 Ma and were metamorphosed during ~2515–2495 Ma (Table 1 and Figure S2). Therefore, the potassic granitoid gneisses in the Northern Liaoning Terrane were crystallized episodically between 2580 and 2515 Ma (~2580 Ma, ~2554–2550 Ma, ~2546–2542 Ma, and ~2529–2515 Ma), with each magmatic episode (especially the first three episodes) following on from the emplacement of spatially associated TTG gneisses. They record metamorphic events at ~2554 Ma, ~2515–2495 Ma, and possibly ~2193 Ma.

4.4. Zircon Lu-Hf Isotopes

Zircon Lu-Hf isotopes of 25 dated samples were calculated at their respective formation ages (Figure 5). Rocks older than 2530 Ma show $\varepsilon Hf(t)$ values close to the depleted mantle evolution line: (1) metavolcanic rock

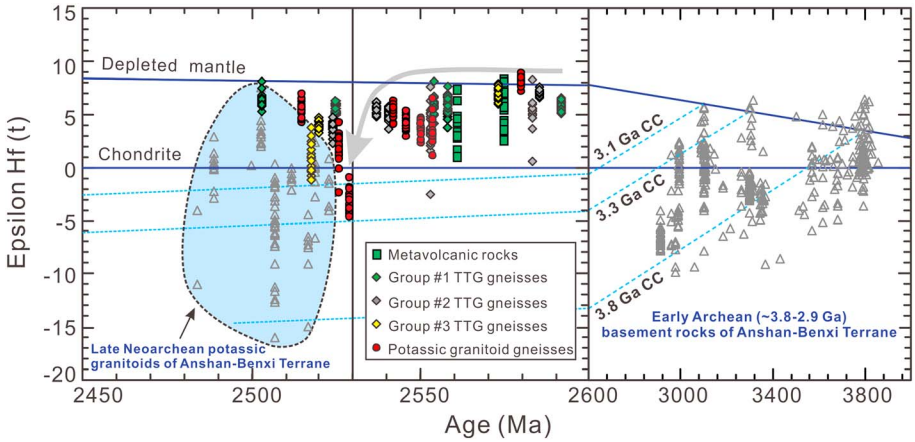

Figure 5. Variation plot of zircon εHf(*t*) values over time for Neoarchean basement rocks in the Northern Liaoning Terrane, showing that the dominant juvenile zircon εHf(*t*) values for rocks older than 2530 Ma contrast with the variable εHf(*t*) of post-2530 Ma rocks. The different groups of TTG gneisses are illustrated below. Zircon Lu-Hf isotopes of ~3.8–2.9 Ga rocks and ~2.5 Ga syenogranites in the Anshan-Benxi terrane are shown for comparison [*Wan et al*., 2013, 2015]. CC, continental crust.

samples (12LN39-3 and 12LN76-2) have εHf(*t*) of +1.0 to +8.3; (2) TTG gneisses (2595–2537 Ma) yield εHf(*t*) largely in the range of +0.5 to +8.2 with T_{DM}(Hf) from 2867 to 2571 Ma, except for a low εHf(*t*) of −2.5 for spot 12LN15-1-03; and (3) potassic granitoids (2580–2542 Ma) show εHf(*t*) of +1.0 to +8.7 and T_{DM}(Hf) of 2844–2548 Ma. Rocks younger than 2530 Ma display more variable εHf(*t*) and T_{DM}(Hf) of −4.7 to +8.1 and 3015–2505 Ma.

5. Geochemical Characters of the Northern Liaoning Terrane

Metavolcanic rocks are basaltic to andesitic in composition (including data of *Peng et al*. [2015]; Figures 6a and 6b and S3). They experienced dominantly amphibolite facies metamorphism, and the prefix "meta" is implicit below. The basalts belong to the tholeiitic series and display nearly flat chondrite-normalized rare earth element (REE) patterns and negative Nb-Ta-Ti anomalies on a primitive mantle (PM)-normalized plot with $(Nb/La)_{PM}$ of 0.26–0.90 (higher $(Nb/La)_{PM}$ of 1.14 of W15FS11-4) (Figures S3c and S3d). The andesites are calc-alkaline, showing mildly fractionated REEs and negative Nb-Ta-Ti anomalies with low $(Nb/La)_{PM}$ of 0.11–0.56 (Figures S3e and S3f).

For the tonalitic-trondhjemitic gneisses (Figures 6c and 6d), 13 samples are excluded as showing low (<62%) or high (>75%) silica or high MgO (>2.5%) and are not considered as typical TTGs [e.g., *Moyen*, 2011] (Figure S4). The remaining 56 samples have high Na_2O (3.39–7.06%) and low K_2O/Na_2O (<0.56). On the chondrite-normalized REE plot, they are divided into three chemical groups, i.e., Groups #1, #2, and #3, which show a diversity of fractionated REE patterns with distinct $(La/Yb)_N$, $(Gd/Yb)_N$, Sr/Y, and Eu anomalies (Figures 7a and S4). They also display negative Nb-Ta-Ti and positive Zr-Hf anomalies (Figure 7b), and most have Nb/Ta (2.84–21.77) comparable with values of associated metavolcanic rocks (1.81–21.09), despite minor high Nb/Ta (23.77–35.86) samples.

Potassic granitoids are monzogranites or syenogranites with minor granodiorites (Figures 6c and 6d). They belong to the high-K calc-alkaline to shoshonite series and have high SiO_2 (63.85–78.48%), K_2O (2.38–8.31%), and K_2O/Na_2O (0.72–3.78). They show variable chondrite-normalized REE patterns and display negative Nb-Ta-Ti and P, positive Zr-Hf, but variable Sr anomalies on the PM-normalized plots (Figure S5).

6. Discussion

6.1. Petrogenesis of Representative Lithologies in Northern Liaoning Terrane

The tholeiitic basalts were likely derived from an oxidized mantle source variably metasomatized by slab-derived fluids and subjected to olivine and plagioclase fractionation but without crustal contamination (Figures 6b and S6). The andesites show chemical features resembling those of high-Mg andesites

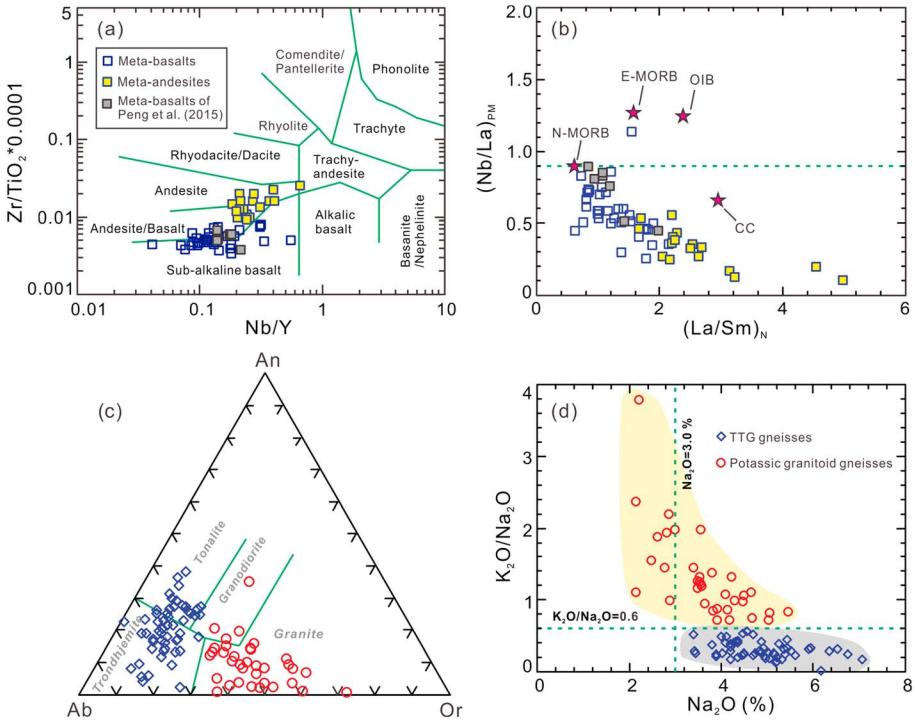

Figure 6. Petrochemical classification and major geochemical features of metavolcanic rocks and granitoid gneisses from Northern Liaoning Terrane: (a) Zr/TiO_2*0.0001 versus Nb/Y plot [*Winchester and Floyd*, 1976]; (b) $(Nb/La)_{PM}$ versus $(La/Sm)_N$ plot [*Sun and McDonough*, 1989]; (c) An-Ab-Or plot [*Barker*, 1979]; and (d) K_2O/Na_2O versus Na_2O plot. Geochemical data of basaltic rocks from Xinbin-Dasuhe area reported by *Peng et al.* [2015] are plotted for comparison.

[*Tatsumi*, 2006], which could have been derived from a hydrous mantle source possibly metasomatized by slab-derived fluids and melts, with clinopyroxene fractionation and plagioclase accumulation (see supporting information for details).

TTG gneisses have chemical features resembling those of experimental melts from mafic rocks, suggesting derivation from crustal sources without input of mantle materials or fractional crystallization (see Text S3.2 in supporting information). TTG gneisses of Groups #1 to #3 show different $(La/Yb)_N$ of 5.13–88.61 (mostly >12), 9.17–50.21, and 2.34–23.54 and Sr/Y of 43.57–315.07, 33.00–118.17, and 4.75–59.40 (Figure S4). Fractionation of garnet, hornblende, or plagioclase are unlikely to account for the chemical diversity of the three groups (supporting information). Modeling reveals that they could have been derived from partial melting of local tholeiitic basalts at varying pressures (Figure 7 and Table S4): Group #1 from ~10–30% melting of (rutile) eclogite (≥15 kbar); Group #2 from ~5–30% melting of garnet-rich amphibolite (~12–15 kbar); and Group #3 from ~5–30% melting of amphibolite (≤10–12 kbar).

Potassic granitoids are also crustal-derived (Figure S5) and show increasingly fractionated REEs with lower Y but higher Sr/Y and Eu anomalies, increasing A/CNK (molar $Al_2O_3/(CaO+Na_2O+K_2O)$) and K_2O/Na_2O, and decreasing CaO and $CaO + FeO_T + MgO + TiO_2$ from ~2580 to 2515 Ma (Figure S7). They could have been derived from progressively enriched crustal sources at increasingly high pressures: ~2580 Ma low-pressure melting of andesites, ~2554–2550 Ma low- to moderate-pressure melting of andesites and greywackes, and ~2546–2542 Ma high-pressure melting of either andesites or pelites and greywackes [*Patiño Douce*, 1999]. Post-2530 Ma rocks were derived from moderate- to high-pressure melting of mixed sources of andesites, TTGs, and greywackes.

6.2. Formation and Stabilization of Continental Crust in the Northern Liaoning Terrane

6.2.1. Pre-2530 Ma Time-Space Magmatic Migration and Cyclic Crustal Formation

Integration of zircon U-Pb isotopic data documented in this study with previously published results indicates that the basement rocks in the Northern Liaoning Terrane formed between ~2.6 and 2.5 Ga (Table 1). Rocks older than 2530 Ma are divided into three spatially and temporally linked episodes of igneous activity, referred to as zones A–C (Figures 1d and 8a). These three zones become young from the southeast to

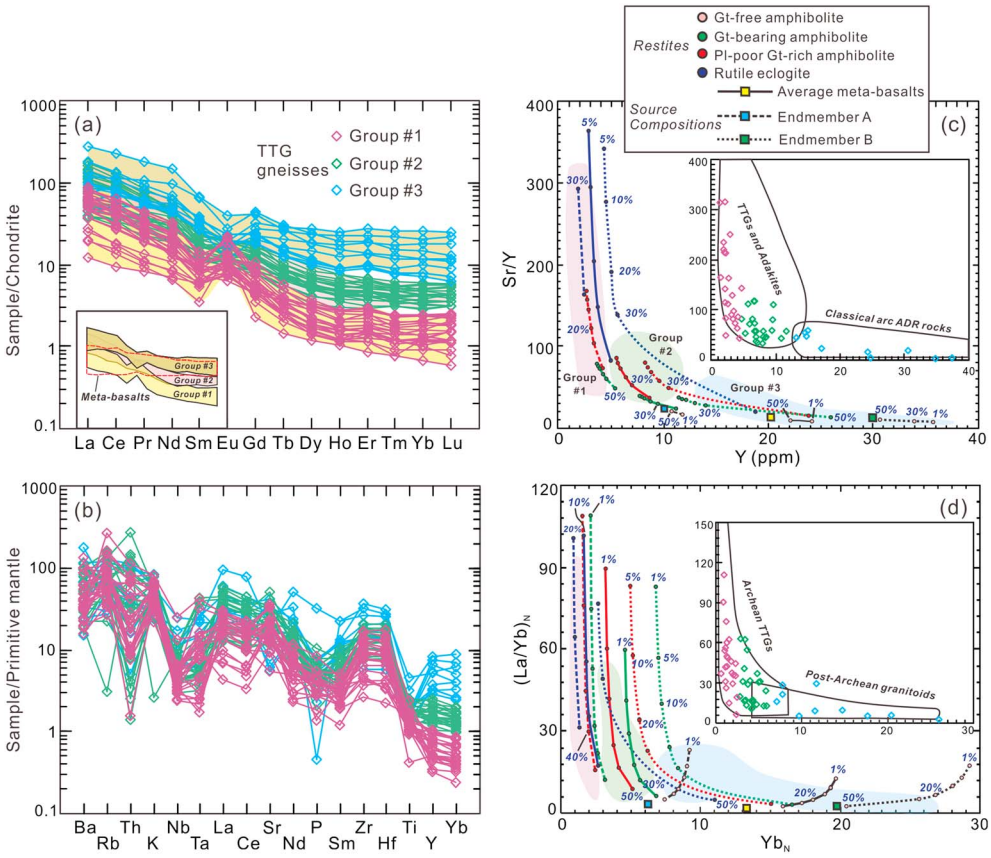

Figure 7. Trace element patterns and genetic modeling of TTG gneisses from Northern Liaoning Terrane: (a, b) chondrite-normalized REE and primitive mantle-normalized multi-element patterns [*Sun and McDonough*, 1989]; (c, d) Sr/Y-Y and $(La/Yb)_N$-Yb_N plots [*Moyen and Martin*, 2012], showing assumed sources (average basaltic rocks and end-members A and B) and modeled batch melting curves under different pressures with residual (rutile) eclogite, garnet (Gt)-rich amphibolite, Gt-bearing amphibolite, and amphibolite. Melting fractions of 1%, 5%, 10%, 20%, 30%, and 50% are labeled for each condition (see modeling parameters and results in Table S4).

northwest, with each displaying a common pattern of magmatic activity resulting in cyclic crust formation followed by its overall stabilization (Figure 9a). Recent studies have highlighted that elemental ratios such as $(La/Yb)_N$ and Sr/Y are sensitive to Moho depth for crustal-derived felsic rocks in modern magmatic arcs provided they did not experience magma fractionation [*Chapman et al*., 2015; *Chiaradia*, 2015]. In this study, we have estimated crustal thickness based on $(La/Yb)_N$ ratios of the TTG gneisses, following the method of *Profeta et al*. [2015] (Figure 8c). In order to avoid the effect of different source compositions, potassic granitoid gneisses were not used in estimates of crustal thickness (Figure 8c), due to the variable involvement of evolved crustal components (e.g., TTG gneisses and metasedimentary rocks) in their sources (Figure S7). The TTG gneisses of Northern Liaoning Terrane have SiO_2 and MgO contents ranging at 63.46–74.65% and 0.36–2.28%, respectively (Table S1). Though the SiO_2 contents are slightly higher than the proposed filtering parameters (SiO_2 at 55–68% and MgO at $<$4%), fractional crystallization and the involvement of mantle materials have been precluded for these TTG gneisses (supporting information) [*Profeta et al*., 2015]. The filtering parameter of Rb/Sr ratio was not used, since granitoid gneisses of Northern Liaoning were subjected to mostly amphibolite and locally granulite facies metamorphism (Figure 2), with probably significant mobilization of Rb. We recognize that this method was developed for modern arcs, not TTG gneisses, and that there are known discrepancies between Archean and Phanerozoic lithospheric rheology and tectonic behavior [*Sizova et al*., 2010; *Gerya*, 2014]. But we also recognize that our results show a consistent evolving temporal pattern in Sr/Y and $(La/Yb)_N$ within each of the three zones of igneous activity in the Northern Liaoning Terrane (Figures 8b and 8c). Thus, although $(La/Yb)_N$ ratios in TTGs are not yet calibrated for application to crustal thickness, the consistent spatial and temporal

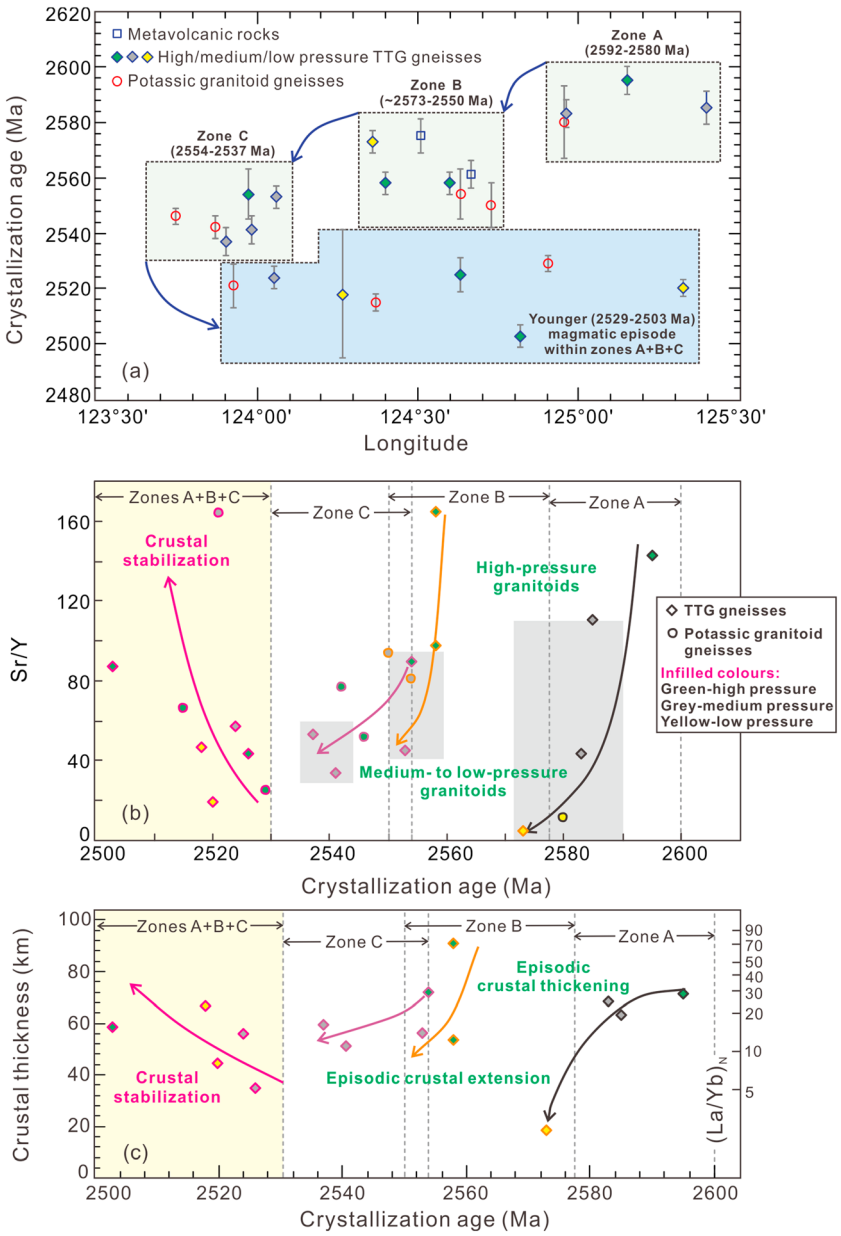

Figure 8. Temporal, spatial, and compositional evolution of Neoarchean granitoid magmatism signifying episodic crustal thickening and extension in the Northern Liaoning Terrane: (a) temporal and spatial distribution of the Neoarchean rocks, showing northwesterly migration of ~2592–2537 Ma granitoid gneisses from Zone A to Zone C. The ~2529–2503 Ma granitoid gneisses were developed throughout the terrane; (b) time-integrated Sr/Y variations of the granitoid gneisses; and (c) plot of variations in $(La/Yb)_N$ of TTG gneisses and calculated crustal thickness over time, indicating episodic crustal thickening and thinning. Crustal thickness was estimated according to the empirical formula of d_m (crustal thickness) = 21.277 ln (1.0204*$(La/Yb)_N$) defined by global correlation between compositions of modern arc felsic rocks and geophysically determined crustal thickness [*Profeta et al.*, 2015]. In order to avoid the effects of different source compositions, the potassic granitoid gneisses were not applied due to the variable involvement of evolved crustal components (e.g., TTG gneisses and metasedimentary rocks) in the sources (Figure S7).

changes in these ratios within the TTG and potassic granitoid gneisses is in accord with evolving patterns of crustal thickening and thinning across the Northern Liaoning Terrane (Figure 8c).

Granitoid gneisses of Zone A range from ~2592 to 2580 Ma and are developed in the Dasuhe-Xinbin region (Figure 8a). The oldest plutonic rocks are the ~2592 Ma Hongmiaozi trondhjemitic gneisses. Chemical modeling reveals that they were derived from high-pressure melting of basaltic rocks (Group #1) with

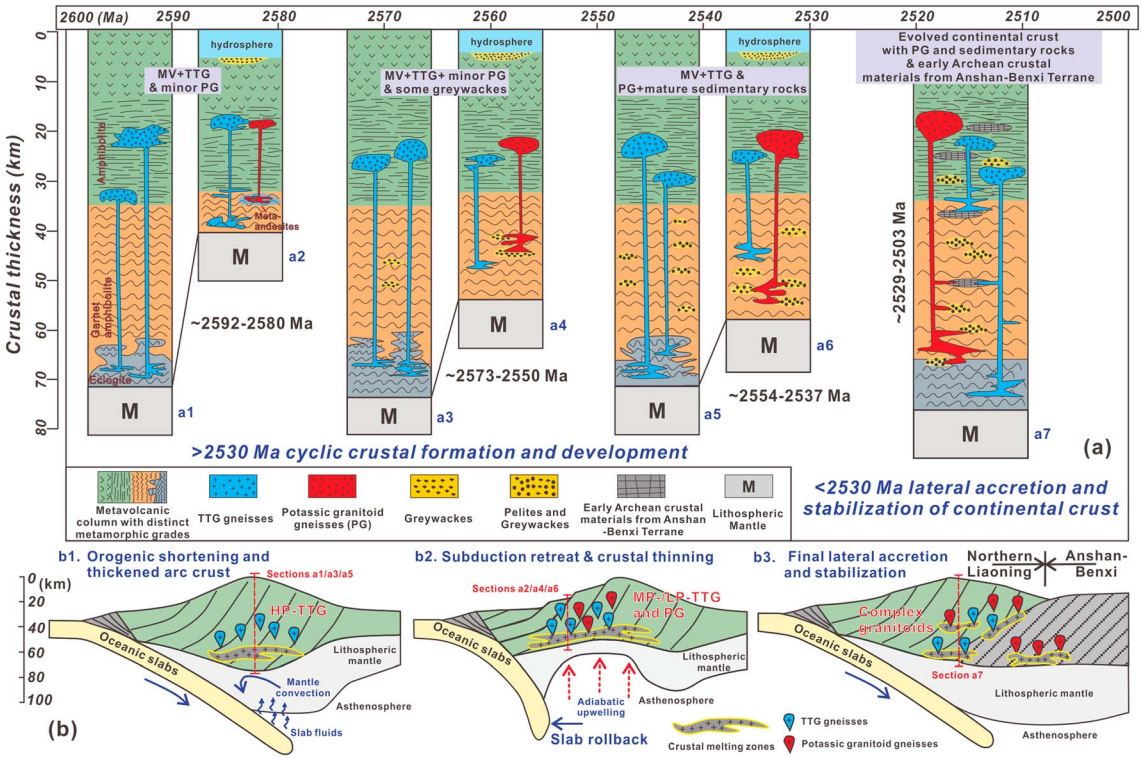

Figure 9. (a) Lithospheric profiles and (b) geodynamic models showing Archean cyclic crustal formation, development, and final stabilization in the Northern Liaoning Terrane. The migration of pre-2530 Ma granitoid magmatism from southeast to northwest is ascribed to episodic crustal (b1) thickening and (b2) thinning that was triggered by cyclic orogenic shortening followed by slab rollback and extension of the overriding plate in an accretionary orogen. During these processes, the crust became progressively more evolved as evidenced by (a1–a6) the increasing involvement of potassic granitoids and sedimentary rocks. (a7) Post-2530 Ma circum-terrane granitoid magmatism and high-grade metamorphism indicate final continental crust stabilization, which are attributed to the lateral accretion of the Northern Liaoning Terrane to the northern continental margin of the Eastern Block represented by the Anshan-Benxi Terrane (b3). MV, basaltic to andesitic metavolcanic rocks; M, mantle; PG, potassic granitoid gneisses.

eclogitic residues but without inputs of mantle materials, implying formation at the base of a thickened crust (Figure 7). In contrast, ~2585–2580 Ma trondhjemitic (Group #2) and monzogranitic gneisses were generated by moderate to low-pressure melting of basaltic and andesitic rocks. Sr/Y ratios of these granitoids decrease from 143.13 to 11.56 (Figure 8b). They are compatible with the decreasing $(La/Yb)_N$ ratios (28.29–19.38) of ~2592–2583 Ma TTG gneisses, suggesting thinning of regional crust from ~72 km to <64 km based on analogies with modern magmatic arcs (Figure 8c). Moreover, felsic rocks older than 2580 Ma are mostly TTG gneisses with limited potassic granitoids (Figure 1). They are metaluminous with depleted zircon ƐHf (*t*), indicating that sedimentary rocks were not involved in the sources of these granitoids (Figure 5). Thus, basaltic to andesitic metavolcanic rocks and TTG gneisses are the major crustal components at this period, with few if any potassic granitoids and sedimentary successions (Figure 9a).

Zone B granitoid gneisses occur in the Xianjinchang-Hongtoushan-Weiziyu region and range in age from ~2573 to 2550 Ma (Figure 8a). Chemical modeling suggests that ~2573 Ma Nanzamu trondhjemitic gneisses formed by partial melting of basaltic rocks at a low pressure (Group #3), whereas ~2558 Ma trondhjemitic gneisses at Baiqizhai and Xiajiabao were generated by partial melting of basaltic rocks at much higher pressures (Group #1) (Figure 7). Monzogranitic to syenogranitic gneisses emplaced at ~2554–2550 Ma around Weiziyu were produced by moderate pressure melting of andesites with some greywackes (Figure S7). Sr/Y ratios of the Zone B granitoids evolve from 4.75, through 98.01–164.31, to 80.61–93.85 (Figure 8b). This implies that the crust could have been thickened (> 70 km) during ~2573–2558 Ma and then thinned to ~56 km at ~2553 Ma, as calculated from the changing $(La/Yb)_N$ ratios from 2.34, through 12.19–72.29, to 13.76 (Figure 8c). Greywackes are modeled in the sources of granitoid magmatism, and biotite plagioclase leptynite and biotite gneisses occur interlayered with metavolcanic rocks [*Zhu et al.*, 2015]. Thus, there is evidence for the inclusion of juvenile sedimentary successions in the crustal profile between ~2573 and 2550 Ma (Figure 9a).

The third granitoid episode, corresponding with Zone C, occurred at ~2554–2537 Ma and is located around Fushun (Figure 8a). Chemical modeling indicates that ~2554 Ma tonalitic gneisses (Group #1) were produced by high-pressure melting of regional basaltic rocks, whereas ~2553–2537 Ma tonalitic to trondhjemitic gneisses (Group #2) formed by partial melting of basaltic rocks at moderate pressures (Figure 7). As calculated from the decreasing $(La/Yb)_N$ of the Zone C TTG gneisses (from 29.08 to 10.94–15.97), regional crustal thickness decreased from ~72 km to ~55 km (51–59 km), which is further supported by decreasing Sr/Y from 89.96 to 53.14 (Figures 8b and 8c). Potassic granitoid gneisses with ages of ~2546–2542 Ma occur from Huiyuan to Shiwen and were derived from mixed sources of andesitic rocks, greywackes, and pelitic rocks at high melting pressures (Figure S7). This implies that voluminous sedimentary rocks may have been recycled to the middle to lower crust, and the crust became more evolved with considerable potassic granitoids and mature sedimentary materials (Figure 9a).

6.2.2. Post-2530 Ma Stabilization of Continental Crust

Granitoid gneisses, including monzogranitic and coeval TTG gneisses (Figure 8a), ranging in age from ~2529 to 2503 Ma, are dispersed throughout the Northern Liaoning Terrane and thus show a much broader distribution than each episode of the older gneisses. These granitoids have variable zircon $\varepsilon Hf(t)$ values (Figure 5). Trondhjemitic gneisses 12LN16-1, 13LB26-5, and 13LB46-5 have depleted zircon $\varepsilon Hf(t)$ (+2.3 to +8.1) and were derived from moderate to high-pressure melting of basaltic rocks. Tonalitic gneisses 12LN27-1 and 13LB12-3 show variable zircon $\varepsilon Hf(t)$ (−1.3 to +4.7), which were generated by low-pressure melting of basaltic rocks. Monzogranitic gneisses 12LN01-1, 12LN59-1, and 12LN80-1 were derived from mixed sources of andesitic rocks, TTGs, and greywackes at moderate to high pressures, showing highly variable zircon $\varepsilon Hf(t)$ of −4.7 to +6.9. These data indicate that a range of crustal materials at distinct crustal levels were subjected to anatexis. The increasing Sr/Y (19.13–86.90) and $(La/Yb)_N$ (5.13–22.82) of the post-2530 Ma granitoids suggest that the crust was thickened (~35 km to ~67 km) (Figures 8b and 8c) [*Profeta et al*., 2015]. This corresponds with regional high-grade metamorphism between ~2530 and 2470 Ma [*W. Wang et al*., 2016], suggesting that the continental crust in the region was finally stabilized (Figure 9a). The widespread emplacement of late Neoarchean potassic granitoid gneisses is consistent with the tectonic models for the Eastern Block of the North China Craton that was stabilized by the end of the Archean [*Liu et al*., 2006; *Kusky*, 2011; *Wan et al*., 2012; *Zhao et al*., 2012; *Kusky et al*., 2016].

6.3. Tectonic Mechanisms of Cyclic Continental Crust Formation

6.3.1. Episodic TTG and Potassic Granitoid Magmatism

TTG and potassic granitoid gneisses in the Northern Liaoning Terrane show a linked spatial, temporal, and compositional distribution (Figures 8 and 9). The site of generation of pre-2530 Ma rocks migrated northwesterly with time, defining three zones (A to C) at ~2592–2580 Ma, ~2573–2550 Ma, and ~2554–2537 Ma. Each zone is dominated by a common litho-tectonic association of early metavolcanic rocks and TTG gneisses succeeded by potassic granitoids. Whereas the TTG gneisses were derived from basaltic rocks, the potassic granitoids display a complex source with variable input from andesitic rocks, TTGs, and juvenile sedimentary rocks (Figures 7 and S7). Furthermore, the TTG and potassic granitoids formed at diverse pressures/crustal levels, with each zone showing magmatic evolution from early high-pressure to late medium- to low-pressure rocks. Episodic variations of Sr/Y and $(La/Yb)_N$ for the granitoids imply a common pattern in each zone of crustal thickening followed by extension (Figures 8b and 8c).

6.3.2. Late Neoarchean Accretionary Orogen and Continental Growth

The granitoid gneisses in the Northern Liaoning Terrane intrude regional metavolcanic rocks (Figure 2). These tholeiitic to calc-alkaline basalts and andesites record slab-mantle wedge interactions, suggesting a supra-subduction zone setting (Figure S6) [*Manikyamba et al*., 2015]. Widespread occurrence of VMS-type Cu-Zn deposits are also hallmarks of accretionary orogens (Figure 1d) [*Huston et al*., 2010]. All these features are reminiscent of Neoproterozoic to Phanerozoic accretionary orogens [*Cawood et al*., 2009]. Episodic crustal thickening and thinning in an accretionary system provides a mechanism to explain the emplacement of granitoids and thus formation and stabilization of continental crust (Figure 9b) [*Cawood*, 2005].

The early high-pressure TTGs within each of the three zones formed by crustal anatexis with residual eclogite, indicating tectonically thickened crust, possibly in the range of 60–70 km based on application of $(La/Yb)_N$ from modern arcs as a proxy for crustal thickness (Figure 8c). Regional consideration suggests that the >2.7 Ga Anshan-Benxi-Tonghua-Helong complexes lie to the south and east of the Northern Liaoning Terrane (Figure 1c). Together with the northwestward migration of granitoid magmatism across

the terrane (Figure 8), and structural data for top-to-the-northwest thrusting (Figures 1d and S1), it is suggested that a SE-dipping subduction resulted in coupling with, and crustal thickening of, the terrane in an upper plate configuration (advancing accretionary orogen) (Figure 9b) [*Cawood et al*., 2009; *Kemp et al*., 2009; *Wang et al*., 2015].

Within each magmatic zone of Northern Liaoning Terrane, the late medium-/low-pressure TTGs and potassic granitoids overlap with or are located to the northwest of the early high-pressure TTGs (Figure 8a) and formed during transition from crustal thickening to thinning (crustal thickness of ~20–50 km). These changes can be attributed to slab rollback and extension of the overriding plate (Figure 9b, retreating accretionary orogen) [*Cawood et al*., 2009]. The inferred slab rollback processes are further supported by the development of extensional basins, forming some volcanogenic massive sulfide (VMS-type) Cu-Zn deposits with interlayered metasedimentary rocks (Figure 1d) [*Zhu et al*., 2015]. Some basaltic rocks with limited subduction imprints were chiefly derived from the upwelling asthenospheric mantle, implying intense crustal extension triggered possibly by slab rollback (Figure 6b). Asthenosphere upwelling during crustal extension triggered high thermal gradients, leading to both high-grade metamorphism and anatexis of metavolcanic rocks and metasedimentary rocks sourced from juvenile arc materials. Any metamorphic imprints during these early orogenic cycles (2592–2537 Ma) are difficult to recognize, perhaps due to pervasive post-2530 Ma tectono-thermal events, except for rare ~2580 Ma metamorphic ages at Weiziyu and Southern Jilin Terrane (possible boundary between the ~2.6–2.5 Ga accretionary system and ~2.7 Ga continental margin) and ~2550 Ma metamorphic ages at the boundary between Zone A and Zone B (Figures 1, 3a, and 4g) [*Guo et al*., 2015; *M. J. Wang et al*., 2016].

Temporal and spatial migration in magmatic activity, regional NE-SW structural pattern, and the top-to-the-northwest thrusting (Figures 1d and S1) are consistent with a process of episodic orogenic shortening followed by slab rollback and extension of the overriding plate, resulting in the migration in the site of arc magmatism to the north and west across the Northern Liaoning Terrane. Periods of lithospheric contraction resulted in thrusting leading to crustal thickening and uplift (Figure 9b). This resulted in erosion and recycling of sedimentary materials, leading to a gradually evolved and thickened crust system, as further supported by the increasing melting pressures of potassic granitoids and the involvement of sedimentary materials in the source (Figures 8b and S7). Notably, there are some temporal or spatial overlaps among different magmatic zones (Figure 8). These have been also observed in the Phanerozoic accretionary orogenic system, e.g., Terra Australis Orogen in Eastern Australia [*Collins and Richards*, 2008; *Cawood et al*., 2009].

Although the Northern Liaoning Terrane adjoins the ~3.8–2.9 Ga Anshan-Benxi and ~2.7 Ga Southern Jilin terranes (Figure 1), ancient crustal materials do not appear to have been involved in the pre-2530 Ma rocks (Figure 5), implying significant crustal growth in an off-craton accretionary system [*W. Wang et al*., 2015, 2016]. After prolonged lateral accretion, post-2530 Ma circum-terrane granitoid magmatism with variable zircon $\varepsilon Hf(t)$ occurred coevally with high-grade metamorphism and resemble the ~2.5 Ga syenogranites at Anshan-Benxi terrane [*Wan et al*., 2015]. Thus, the Northern Liaoning Terrane likely accreted onto the northern continental margin of NCC after ~2530 Ma, marking final stabilization of the regional continental crust (Figure 9b). Similarly, a late Neoarchean intra-oceanic arc system was proposed for the region southwest of Northern Liaoning Terrane (Western Liaoning, Zunhua-Qinglong Block of Eastern Hebei, and Wutai Complex), which accreted onto the $>$2.7 Ga continental nucleus of Eastern Block at the end of the Archean [*Liu et al*., 2006; *W. Wang et al*., 2011, 2015, 2016, 2017; *Guo et al*., 2013].

6.4. Temporal Trends in Archean Granitoids, Accretionary Orogens, and Supercontinents

Granitoid gneisses are major components of Archean terranes and display complex chemical features, especially those of TTGs [*Hoffmann et al*., 2011; *Moyen*, 2011]. In this study, we recompiled Moyen's data on TTGs, and suggest that low- to medium-pressure TTGs occurred (semi-)continuously since ~3.8 Ga, whereas high-pressure TTGs only appear continuously in the rock archive after ~3.1 Ga (Figure 10). Potassic granitoids of the sanukitoid series along with crustal-derived granodiorites and monzogranites were produced within most cratons since ~3.0 Ga [*Laurent et al*., 2014]. Notably, the late Archean granitoids are distinct from felsic rocks formed in stagnant-lid/plume settings, with the latter showing less fractionated REE patterns [*Debaille et al*., 2013; *Reimink et al*., 2014]. Rather, they resemble the episodic granitoids of Northern Liaoning Terrane, and are therefore interpreted to form in an accretionary orogen with high-pressure

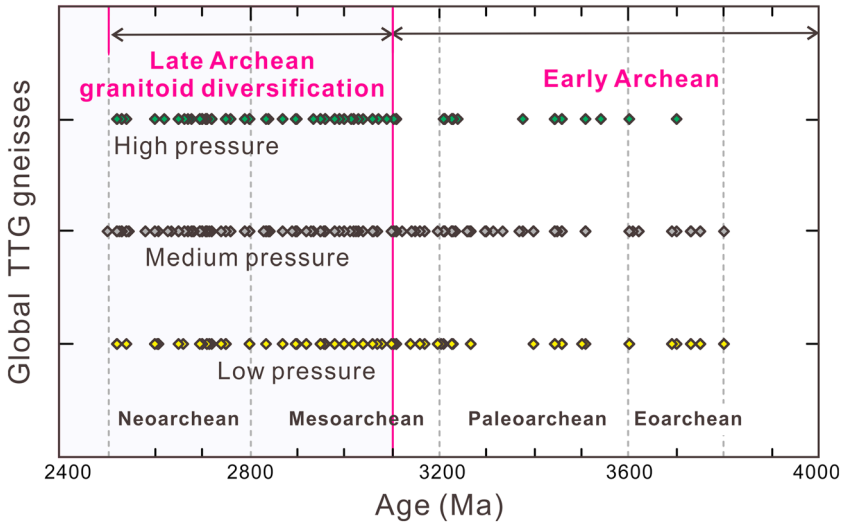

Figure 10. Distribution of globally different types of TTG gneisses over time [*Moyen*, 2011]. While low- to medium-pressure TTGs occurred (semi)continuously since ~3.8 Ga, continuous high-pressure TTGs appeared only after ~3.1 Ga. This indicates global granitoid diversification after ~3.0 Ga, i.e., both high-/medium-/low-pressure TTG and sanukitoids and granodioritic-monzogranitic gneisses [*Laurent et al*., 2014], possibly reflecting late Archean onset of accretionary orogeny globally [*Cawood et al*., 2009].

TTGs formed during orogenic thickening, whereas medium-/low-pressure TTGs and potassic granitoids generated during crustal extension due to slab rollback (Figure 9b). Recent metamorphic, geochemical, and thermal modeling studies endorse the onset of plate tectonics and associated accretionary orogens by 3.2–3.0 Ga [*Cawood et al*., 2006; *Brown*, 2014; *Gerya*, 2014; *Hawkesworth et al*., 2016]. Collectively, the diversification of granitoids started globally at ~3.0 Ga, recording vigorous crust-mantle interactions possibly within a mobile-lid Earth system [*Halla et al*., 2017].

With intense late Archean lateral accretion, global continental crust was emplaced by increasingly more and diversified granitoids, which became thickened and increasingly felsic and potassic [*Dhuime et al*., 2015; *Tang et al*., 2016]. These processes yielded a more Phanerozoic-like continental crust that is conducive to large-scale lateral accretion, which could finally lead to the assembly of late Archean supercontinents [*Bleeker*, 2003; *Condie and Kröner*, 2013]. Examples include the Eastern Block of NCC, India, Tarim, South Australia, East Antarctica, and Rae/Sask cratons (Canada), which mutually record ~2.6–2.5 Ga lateral accretion processes and were stabilized by the end of the Archean [*W. Wang et al*., 2016].

7. Conclusions

1. Granitoid gneisses of Northern Liaoning Terrane formed at ~2592–2503 Ma and show linked temporal, spatial, and compositional evolution. Between ~2592 and 2537 Ma magmatic activities migrated from southeast to northwest across the terrane, defining three zones with each showing a common evolution from high-pressure TTGs to medium-/low-pressure TTGs and potassic granitoids. Between ~2529 and 2503 Ma potassic granitoids and TTG gneisses were emplaced throughout the terrane. While TTG gneisses were derived from partial melting of tholeiitic basaltic rocks at high, moderate, and low pressures, the potassic granitoid gneisses were sourced from evolved crustal sources involving different proportions of metamorphosed andesitic and sedimentary rocks, and TTG gneisses.
2. The Northern Liaoning Terrane witnessed episodic late Neoarchean crustal thickening and extension, and the early crust, consisting dominantly of metavolcanic rocks and TTG gneisses, displays increasing involvement of sedimentary rocks and potassic granitoids. Post-2530 Ma circum-terrane granitoid magmatism and high-grade metamorphism signify final crustal stabilization, forming highly evolved continental crust with large volumes of potassic granitoids, sedimentary rocks, and ancient crustal materials.
3. The cyclic record of crust formation, development, and final stabilization in the Northern Liaoning Terrane evolved in an Archean accretionary orogen with a SE-dipping subduction polarity, which underwent cyclic orogenic thickening followed by slab rollback and extension of the overriding plate. This accretionary

system records ~2.6–2.5 Ga lateral crustal growth and was accreted to the northern continental margin of Eastern Block of the North China Craton after ~2530 Ma.

4. Accretionary orogens could have contributed significantly to late Archean continental formation and stabilization, resulting in both the diversification of granitoid magmatism and supercontinent assembly by the end of the Archean.

Acknowledgments

We would like to express our thanks to Editor Nathan A. Niemi and Associate Editor Mihai Ducea, Tim Kusky, and one anonymous reviewer, whose constructive suggestions and comments have led to significant improvements in the quality of this manuscript. We also appreciate laboratory assistance provided by L. Su at the Geological Lab Center, China University of Geosciences (Beijing), and Z.C. Hu at the State Key Laboratory of Geological Processes and Mineral Resources, China University of Geosciences (Wuhan). This study is financially supported by the National Natural Science Foundation of China (grants 41502179, 41530207, 41472165) and Central University Basic Scientific Research Business Expenses of China University of Geosciences (Beijing) (grants 2652015038 and 2-9-2016-006). P.A.C. acknowledges support from Australian Research Council grant FL160100168. All analytical results are presented in the supporting information, and the original data are available upon request from the first author. This is CUGB petro-geochemical contribution PGC-201523.

References

Bai, X., S. W. Liu, L. F. Zhang, M. Yan, W. Wang, R. R. Guo, and B. R. Guo (2014), Geological event series of Early Precambrian complex in South Fushun area, Liaoning Province [in Chinese with English abstract], *Acta Petrol. Sin.*, *30*, 2905–2924.

Barker, F. (1979), Trondhjemite: Definition, environment and hypotheses of origin, in *Trondhjemites, Dacites, and Related Rocks*, edited by F. Barker, pp. 1–312, Amsterdam, doi:10.1016/B978-0-444-41765-7.510006-X.

Bleeker, W. (2003), The late Archean record: A puzzle in ca. 35 pieces, *Lithos*, *71*, 99–134, doi:10.1016/j.lithos.2003.07.003.

Brown, M. (2014), The contribution of metamorphic petrology to understanding lithosphere evolution and geodynamics, *Geosci. Front.*, *5*, 553–569, doi:10.1016/j.gsf.2014.02.005.

Cawood, P. A., C. J. Hawkesworth, and B. Dhuime (2013), The continental record and the generation of continental crust, *Geol. Soc. Am. Bull.*, *125*, 14–32, doi:10.1130/B30722.1.

Cawood, P. A., A. Kröner, W. J. Collins, T. M. Kusky, W. D. Mooney, and B. F. Windley (2009), Earth accretionary orogens through Earth history, in *Earth Accretionary Systems in Space and Time*, edited by P. A. Cawood and A. Kröner, *Geol. Soc. London, Spec. Publ., 318*, 1–36, doi:10.1144/SP318.1.

Cawood, P. A., A. Kröner, and S. Pisarevsky (2006), Precambrian plate tectonics: Criteria and evidence, *GSA Today*, *16*, 4–11, doi:10.1130/GSAT01607.1.

Cawood, P. A. (2005), Terra Australis Orogen: Rodinia breakup and development of the Pacific and Iapetus margins of Gondwana during the Neoproterozoic and Paleozoic, *Earth Sci. Rev.*, *69*, 249–279, doi:10.1016/j.earscirev.2004.09.001.

Chapman, J. B., M. N. Ducea, P. G. DeCelles, and L. Profeta (2015), Tracking changes in crustal thickness during orogenic evolution with Sr/Y: An example from the North American Cordillera, *Geology*, *43*, 919–922, doi:10.1130/G36996.1.

Chiaradia, M. (2015), Crustal thickness control on Sr/Y signatures of recent arc magmas: An Earth scale perspective, *Sci. Rep.*, *5*, 1–5, doi:10.1038/srep08115.

Collins, W. J., and S. W. Richards (2008), Geodynamic significance of S-type granites in circum-Pacific orogens, *Geology*, *36*, 559–562, doi:10.1130/G24658A.1.

Condie, K. C. (2014), How to make a continent: Thirty-five years of TTG research, in *Evolution of Archean Crust and Early Life, Modern Approaches to Solid Earth Sciences*, vol. 7, edited by Y. Dilek and H. Furnes, pp. 179–193, Springer Science, Dordrecht, Netherlands, doi:10.1007/978-94-007-7615-9_7.

Condie, K. C., and A. Kröner (2013), The building blocks of continental crust: Evidence for a major change in the tectonic setting of continental growth at the end of the Archean, *Gondwana Res.*, *23*, 394–402, doi:10.1016/j.gr.2011.09.011.

Debaille, V., C. O'Neill, A. D. Brandon, P. Haenecour, Q. Z. Yin, N. Mattielli, and A. H. Treiman (2013), Stagnant-lid tectonics in early Earth revealed by ^{142}Nd variations in late Archean rocks, *Earth Planet. Sci. Lett.*, *373*, 83–92, doi:10.1016/j.epsl.2013.04.016.

Deng, H., T. Kusky, A. Polat, J. P. Wang, L. Wang, J. M. Fu, Z. S. Wang, and Y. Yuan (2014), Geochronology, mantle source composition and geodynamic constraints on the origin of Neoarchean mafic dykes in the Zanhuang Complex, central Orogenic Belt, North China Craton, *Lithos*, *205*, 359–378, doi:10.1016/j.lithos.2014.07.011.

Dhuime, B., A. Wuestefeld, and C. J. Hawkesworth (2015), Emergence of modern continental crust about 3 billion years ago, *Nat. Geosci.*, *8*, 552–555, doi:10.1038/NGEO2466.

Foley, S., M. Tiepolo, and V. Riccardo (2002), Growth of early continental crust controlled by melting of amphibolite in subduction zones, *Nature*, *417*, 837–840, doi:10.1038/nature00799.

Gerya, T. (2014), Precambrian geodynamics: Concepts and models, *Gondwana Res.*, *25*, 442–463, doi:10.1016/j.gr.2012.11.008.

Guo, B. R., S. W. Liu, J. Zhang, and M. Yan (2015), Zircon U-Pb-Hf isotope systematics and geochemistry of Helong granite-greenstone belt in southern Jilin Province, China: Implications for Neoarchean crustal evolution of the northeastern margin of North China Craton, *Precambrian Res.*, *271*, 254–277, doi:10.1016/j.precamres.2015.10.009.

Guo, B. R., S. W. Liu, J. Zhang, W. Wang, J. H. Fu, and M. J. Wang (2016), Neoarchean Andean-type active continental margin in the northeastern North China Craton: Geochemical and geochronological evidence from metavolcanic rocks in the Jiapigou granite-greenstone belt, southern Jilin Province, *Precambrian Res.*, *285*, 147–169, doi:10.1016/j.precamres.2015.10.009.

Guo, R. R., S. W. Liu, M. Santosh, Q. G. Li, X. Bai, and W. Wang (2013), Zircon U-Pb-Hf isotopes and geochemistry of Neoarchean dioritic-trondhjemitic gneisses, eastern Hebei, North China Craton: Constraints on petrogenesis and tectonic implications, *Gondwana Res.*, *24*, 664–686, doi:10.1016/j.gr.2012.12.025.

Halla, J., M. J. Whitehouse, T. Ahmad, and Z. Bagal (2017), Archaean granitoids: An overview and significance from a tectonic perspective, in *Crust-Mantle Interactions and Granitoid Diversification: Insights from Archaean Cratons*, edited by J. Halla et al., *Geol. Soc. London, Spec. Publ., 449*, 1–18, doi:10.1144/SP449.10.

Hawkesworth, C., P. A. Cawood, and B. Dhuime (2016), Tectonics and crustal evolution, *GSA Today*, *26*, 4–11, doi:10.1130/GSATG272A.1.

Hoffmann, J. E., C. Münker, T. Naeraa, M. Rosing, D. Herwartz, D. Garbe-Schöberg, and H. Svahnberg (2011), Mechanisms of Archean crust formation inferred from high-precision HFSE systematics in TTGs, *Geochim. Cosmochim. Acta*, *75*, 4157–4178, doi:10.1016/j.gca.2011.04.027.

Huston, D. L., S. Pehrsson, B. M. Eglington, and K. Zaw (2010), The geology and metallogeny of volcanic-hosted massive sulfide deposits: Variations through geologic time and with tectonic setting, *Econ. Geol.*, *105*, 571–591, doi:10.2113/gsecongeo.105.3.571.

Jahn, B. M., F. Y. Wu, and B. Chen (2000), Granitoids of the central Asian Orogenic Belt and continental growth in the Phanerozoic, *Trans. R. Soc. Edinb. Earth Sci.*, *91*, 181–193, doi:10.1017/S0263593300007367.

Kemp, A. I. S., C. J. Hawkesworth, W. J. Collins, C. M. Gray, and EIMF (2009), Isotopic evidence for rapid continental growth in an extensional accretionary orogen: The Tasmanides, eastern Australia, *Earth Planet. Sci. Lett.*, *284*, 455–466, doi:10.1016/j.epsl.2009.05.011.

Korenaga, J. (2013), Initiation and evolution of plate tectonics on Earth: Theories and observations, *Annu. Rev. Earth Planet. Sci.*, *41*, 117–151, doi:10.1146/annurev-earth-050212-124208.

Kusky, T. M., et al. (2016), Insights into the tectonic evolution of the North China Craton through comparative tectonic analysis: A record of outward growth of Precambrian continents, *Earth Sci. Rev.*, *162*, 387–432, doi:10.1016/j.earscirev.2016.09.002.

Kusky, T. M. (2011), Geophysical and geological tests of tectonic models of the North China Craton, *Gondwana Res.*, *20*, 26–35, doi:10.1016/j.gr.2011.01.004.

Laurent, O., H. Martin, J. F. Moyen, and R. Doucelance (2014), The diversity and evolution of late-Archean granitoids: Evidence for the onset of "modern-style" plate tectonics between 3.0 and 2.5 Ga, *Lithos*, *205*, 208–235, doi:10.1016/j.lithos.2014.06.012.

Liu, S. W., G. C. Zhao, S. A. Wilde, G. M. Shu, M. Sun, Q. G. Li, W. Tian, and J. Zhang (2006), Th-U-Pb monazite geochronology of the Lüliang and Wutai Complexes: Constraints on the tectonothermal evolution of the trans-North China Orogen, *Precambrian Res.*, *148*, 205–225, doi:10.1016/j.precamres.2006.04.003.

Manikyamba, C., S. Ganguly, M. Santosh, A. Saha, A. Chatterjee, and A. C. Khelen (2015), Neoarchean arc-juvenile back-arc magmatism in eastern Dharwar craton, India: Geochemical fingerprints from the basalts of Kadiri greenstone belt, *Precambrian Res.*, *258*, 1–23, doi:10.1016/j.precamres.2014.12.003.

Martin, H., R. H. Smithies, J. F. Moyen, and D. Champion (2005), An overview of adakite, tonalite-trondhjemite-granodiorite (TTG), and sanukitoid: Relationships and some implications for crust evolution, *Lithos*, *79*, 1–24, doi:10.1016/j.lithos.2004.04.048.

Martin, H., J. F. Moyen, M. Guitreau, J. Blichert-Toft, and J. F. Le Pennec (2014), Why Archaean TTG cannot be generated by MORB melting in subduction zones, *Lithos*, *198-199*, 1–13, doi:10.1016/j.lithos.2014.02.017.

Moyen, J. F. (2011), The composite Archaean grey gneisses: Petrological significance, and evidence for a non-unique tectonic setting for Archaean crustal growth, *Lithos*, *123*, 21–36, doi:10.1016/j.lithos.2010.09.015.

Moyen, J. F., and H. Martin (2012), Forty years of TTG research, *Lithos*, *148*, 312–336, doi:10.1016/j.lithos.2012.06.010.

Nutman, A. P., Y. S. Wan, L. L. Du, C. R. L. Friend, C. Y. Dong, H. Q. Xie, W. Wang, H. Y. Sun, and D. Y. Liu (2011), Multistage late Neoarchaean crustal evolution of the North China Craton, eastern Hebei, *Precambrian Res.*, *189*, 43–65, doi:10.1016/j.precamres.2011.04.005.

Patiño Douce, A. E. (1999), What do experiments tell us about the relative contributions of crust and mantle to the origin of granitic magmas?, in *Understanding Granites: Integrating New and Classic Techniques*, edited by A. Castro, C. Fernandez, and J. L. Vigneresse, *Geol. Soc. London, Spec. Publ., 168*, 55–75, doi:10.1144/GSL.SP.1999.168.01.05.

Peng, P., C. Wang, X. P. Wang, and S. Y. Yang (2015), Qingyuan high-grade granite-greenstone terrain in the eastern North China Craton: Root of a Neoarchaean arc, *Tectonophysics*, *662*, 7–21, doi:10.1016/j.tecto.2015.04.013.

Phillips, G., B. Landenberger, and E. A. Belousva (2011), Building the New England batholith, eastern Australia-linking granite petrogenesis with geodynamic setting using Hf isotopes in zircon, *Lithos*, *122*, 1–12, doi:10.1016/j.lithos.2010.11.005.

Profeta, L., M. N. Ducea, J. B. Chapman, S. R. Paterson, S. M. H. Gonzales, M. Kirsch, L. Petrescu, and P. G. DeCelles (2015), Quantifying crustal thickness over time in magmatic arcs, *Sci. Rep.*, *5*, 17,786, doi:10.1016/j.lithos.2010.11.005.

Reimink, J. R., T. Chacko, R. A. Stern, and L. M. Heaman (2014), Earth's earliest evolved crust generated in an Iceland-like setting, *Nat. Geosci.*, *7*, 529–533, doi:10.1038/NGEO2170.

Robinson, F. A., J. D. Foden, A. S. Collins, and J. L. Payne (2014), Arabian shield magmatic cycles and their relationship with Gondwana assembly: Insights from zircon U-Pb and Hf isotopes, *Earth Planet. Sci. Lett.*, *408*, 207–225, doi:10.1016/j.epsl.2014.10.010.

Santosh, M., E. Shaji, T. Tsunogae, M. R. Mohan, M. Satyanarayanan, and K. Horie (2013), Suprasubduction zone ophiolite from Agali hill: Petrology, zircon SHRIMP U-Pb geochronology, geochemistry and implications for Neoarchean plate tectonics in southern India, *Precambrian Res.*, *21*, 301–324, doi:10.1016/j.precamres.2013.04.003.

Shen, B. F., H. Luo, G. G. Han, X. Y. Dai, W. S. Jin, X. D. Hu, S. B. Li, and S. Y. Bi (1994), *Archean Geology and Metallization in Northern Liaoning Province and Southern Jilin Province* [in Chinese], pp. 1–255, Geol. Publ. House, Beijing.

Sizova, E., T. Gerya, M. Brown, and L. L. Perchuk (2010), Subduction styles in the Precambrian: Insight from numerical experiments, *Lithos*, *116*, 209–229, doi:10.1016/j.lithos.2009.05.028.

Sun, S. S., and W. F. McDonough (1989), Chemical and isotopic systematics of oceanic basalts: Implication for mantle composition and processes, in *Magmatism in Ocean Basins*, edited by A. D. Saunders and M. J. Norry, *Geol. Soc. London, Spec. Publ., 42*, 313–345, doi:10.1144/GSL.SP.1989.042.01.19.

Tang, M., K. Chen, and R. L. Rudnick (2016), Archean upper crust transition from mafic to felsic marks the onset of plate tectonics, *Science*, *351*, 372–375, doi:10.1126/science.aad5513.

Tatsumi, Y. (2006), High-Mg andesites in the Setouchi volcanic belt, southwestern Japan: Analogy to Archean magmatism and continental crust formation?, *Annu. Rev. Earth Planet. Sci.*, *34*, 467–499, doi:10.1146/annurev.earth.34.031405.125014.

Wan, Y. S., B. Song, Y. S. Geng, and D. Y. Liu (2005), Geochemical characteristics of Archean basement in the Fushun-Qingyuan area, northern Liaoning Province and its geological significance [in Chinese with English abstract], *Geol. Rev.*, *51*, 128–137.

Wan, Y. S., C. Y. Dong, D. Y. Liu, A. Kröner, C. H. Yang, W. Wang, L. L. Du, H. Q. Xie, and M. Z. Ma (2012), Zircon ages and geochemistry of late Neoarchean syenogranites in the North China Craton: A review, *Precambrian Res.*, *222–223*, 265–289, doi:10.1016/j.precamres.2011.05.001.

Wan, Y. S., Y. H. Zhang, I. S. Williams, D. Y. Liu, C. Y. Dong, R. L. Fan, Y. R. Shi, and M. Z. Ma (2013), Extreme zircon O isotopic compositions from 3.8 to 2.5 Ga magmatic rocks from the Anshan area, North China Craton, *Chem. Geol.*, *352*, 108–124, doi:10.1016/j.chemgeo.2013.06.009.

Wan, Y. S., S. W. Xie, C. Y. Yang, A. Kröner, M. Z. Ma, C. Y. Dong, L. L. Du, H. Q. Xie, and D. Y. Liu (2014), Early Neoarchean (~2.7 Ga) tectono-thermal events in the North China Craton: A synthesis, *Precambrian Res.*, *247*, 45–63, doi:10.1016/j.precamres.2014.03.019.

Wan, Y. S., M. Z. Ma, C. Y. Dong, H. Q. Xie, S. W. Xie, P. Ren, and D. Y. Liu (2015), Widespread late Neoarchean reworking of Meso- to Paleoarchean continental crust in the Anshan-Benxi area, North China Craton, as documented by U-Pb-Nd-Hf-O isotopes, *Am. J. Sci.*, *315*, 620–670, doi:10.2475/07.2015.02.

Wang, M. J., S. W. Liu, W. Wang, K. Wang, M. Yan, B. R. Guo, X. Bai, and R. R. Guo (2016), Petrogenesis and tectonic implications of the Neoarchean North Liaoning tonalitic-trondhjemitic gneisses of the North China Craton, North China, *J. Asian Earth Sci.*, *131*, 12–39, doi:10.1016/j.jseaes.2016.09.012.

Wang, W., S. W. Liu, P. A. Cawood, X. Bai, R. R. Guo, B. R. Guo, and K. Wang (2016), Late Neoarchean subduction-related crustal growth in the northern Liaoning region of the North China Craton: Evidence from ~2.55 to 2.50 Ga granitoid gneisses, *Precambrian Res.*, *281*, 200–223, doi:10.1016/j.precamres.2016.05.018.

Wang, W., S. W. Liu, X. Bai, P. T. Yang, Q. G. Li, and L. F. Zhang (2011), Geochemistry and zircon U-Pb-Hf isotopic systematics of the Neoarchean Yixian-Fuxin greenstone belt, northern margin of the North China Craton: Implications for petrogenesis and tectonic setting, *Gondwana Res.*, *20*, 64–81, doi:10.1016/j.gr.2011.02.012.

Wang, W., S. W. Liu, M. Santosh, G. H. Wang, X. Bai, and R. R. Guo (2015), Neoarchean intra-oceanic arc system in the western Liaoning Province: Implications for the Early Precambrian crust-mantle geodynamic evolution of the eastern block of the North China Craton, *Earth Sci. Rev.*, *150*, 329–364, doi:10.1016/j.earscirev.2015.08.002.

Wang, W., S. W. Liu, P. A. Cawood, R. R. Guo, X. Bai, and B. R. Guo (2017), Late Neoarchean crust-mantle geodynamics: Evidence from Pingquan complex of the northern Hebei Province, North China Craton, *Precambrian Res.*, doi:10.1016/j.precamres.2017.06.007.

Winchester, J. A., and P. A. Floyd (1976), Geochemical magma type discrimination: Application to altered and metamorphosed basic igneous rocks, *Earth Planet. Sci. Lett.*, *28*, 459–469, doi:10.1016/0012-821X(76)90207-7.

Zhai, M. G., and M. Santosh (2011), The Early Precambrian odyssey of the North China Craton: A synoptic overview, *Gondwana Res.*, *20*, 6–25, doi:10.1016/j.gr.2011.02.005.

Zhao, G. C., P. A. Cawood, S. Z. Li, S. A. Wilde, M. Sun, J. Zhang, Y. H. He, and C. Q. Yin (2012), Amalgamation of the North China Craton: Key issues and discussions, *Precambrian Res.*, *222-223*, 55–76, doi:10.1016/j.precamres.2012.09.016.

Zhu, M. T., L. C. Zhang, Y. P. Dai, and C. L. Wang (2015), In situ zircon U-Pb dating and O isotopes of the Neoarchean Hongtoushan VMS Cu-Zn deposit in the North China Craton: Implication for the ore genesis, *Ore Geol. Rev.*, *67*, 354–367, doi:10.1016/j.oregeorev.2014.12.019.